EFFECT OF GAUSSIAN CURVATURE ON FRICTIONAL INTERACTION BETWEEN AN ULTRA-THIN FILM AND A SOFT-SUBSTRATE

A THESIS

submitted in partial fulfillment of the requirements

for the award of the dual degree of

Bachelor of Science-Master of Science

in

PHYSICS

by

SWADHIN AGRAWAL

(15223)

DEPARTMENT OF PHYSICS
INDIAN INSTITUTE OF SCIENCE EDUCATION AND RESEARCH
BHOPAL
BHOPAL - 462066

May 11, 2020

Indian Institute of Science Education and Research Bhopal
(Established by MHRD, Govt. of India)

CERTIFICATE

This is to certify that **Swadhin Agrawal**, BS-MS (Dual Degree) student in Department of Physics, has completed bonafide work on the thesis entitled **'Effect of Gaussian curvature on frictional interaction between an ultra-thin film and a soft-substrate'** under my supervision and guidance.

May 11, 2020
IISER Bhopal **Dr Deepak Kumar**

Committee Member	Signature	Date

ACADEMIC INTEGRITY AND COPYRIGHT DISCLAIMER

I hereby declare that this project is my own work and due acknowledgement has been made wherever the work described is based on the findings of other investigators. This report has not been accepted for the award of any other degree or diploma at IISER Bhopal or any other educational institution. I also declare that I have adhered to all principles of academic honesty and integrity and have not misrepresented or fabricated or falsified any idea/data/fact/source in my submission.

I certify that all copyrighted material incorporated into this document is in compliance with the Indian Copyright (Amendment) Act (2012) and that I have received written permission from the copyright owners for my use of their work, which is beyond the scope of the law. I agree to indemnify and safeguard IISER Bhopal from any claims that may arise from any copyright violation.

May 11, 2020
IISER Bhopal **Swadhin Agrawal**

ACKNOWLEDGEMENT

I would like to express my gratitude to **Dr Deepak Kumar** for giving me this opportunity to carry out this master thesis under his supervision, for guiding me and getting engaged in the experiments throughout the research work. My special thank to **Prof. Dhanvir Singh Rana**, **Dr Pani Kumar Peddibhotla** and **Dr Venkateshwar Rao Dugyala** for helping me by providing their lab equipment. I would also like to thank **Nitin Kriplani** for introducing me to this problem.

My thanks are also extended to my sponsors, INSPIRE, Department of Science and Technology, MHRD, Govt. of India for their generous funding throughout my graduation.

I am grateful to the Department of Physics and Department of Engineering Sciences, IISER Bhopal for their support and for providing me with the required infrastructure and facilities to complete my graduation and carry out this project.

I would also like to thank my colleagues Vishal Gupta, Razaul Mustafa, Akshat Singhal and Parth Sunil Kumar Naik for important discussions during the study.

Finally, I would like to thank my loved ones, my parents and my family and friends for supporting me throughout the entire process, both by keeping me harmonious and helping me putting pieces together. I will be grateful forever for your love.

Swadhin Agrawal

PREFACE

This thesis gives a brief report about the research work that I have carried out under the guideline of Dr Deepak Kumar in the Department of Physics at the Indian Institute of Science Education and Research, Bhopal from May, 2019 to April, 2020.

Swadhin Agrawal

ABSTRACT

Thin films are widely employed in designing a variety of micro and nano-electro-mechanical devices. The fabrication strategies employed and the device performance both depend crucially on the adhesive and frictional properties of these thin films for a given substrate[1]. In this project, we have explored the role of geometry in modifying the strength of adhesion and friction between a thin film and a substrate of given materials. In our experiments, we loaded an ultra-thin circular polystyrene film on top of a swollen hydrogel sphere, a super absorbent polymer ball which shrinks over time due to evaporation of water. And by measuring the compression and shrinking rate of the film and the substrate respectively through image analysis, we found that the frictional interaction between the substrate and the film depends on the underlying Gaussian curvature[2] of the substrate.

By repeating the experiment on a flat and cylindrical substrate both of which have zero Gaussian curvature but are made from the same material we conclusively demonstrated that the friction gets enhanced with increasing positive Gaussian curvature of the substrate. Following this, we also tested the case of the convex and concave type of positive Gaussian curvatures. Further, on spherical surfaces, the film develops a very specific type of crumpling pattern which gets denser with time. Patterns along with experiment on concave positive Gaussian curvature together directed us to recognize that the direction of elastic stress is responsible for the increase in frictional interaction with an increase in positive convex Gaussian curvature of the substrate. The experiment on positive convex Gaussian curvature also allows us to explore crumpling dynamics without disturbing the experiment by re-opening the crumpled film, hence emerging as a promising experimental approach for future studies on such processes.

LIST OF FIGURES

LIST OF TABLES

Contents

Chapter 1

Introduction

Recently, people have started deploying sheets as sensing tools in MEMS and NEMS devices, which are widely being used in research and industries. Graphene straintronics[1] in which large strains are used to deform graphene and modify the electronic band structure of graphene. Doing this without delamination is a challenging task due to the requirement of high adhesion energies. Nanomechanical switch[1] is another promising technology where strong adhesion reduces the device performance. Such problems are densely populated in the development of MEMS and NEMS technology. Due to the wide range of available material types, deformation patterns diversity and non-linearity in problems involving deformation of 2-D sheets, people are still struggling to understand them in different settings like in presence of a loading force[3], pattern dependence on history of crumpling and directions of forces[4], etc. The non-linearity which encompasses mostly all the problems are being tackled through computational methods. On the same line, our work shows how adhesion can be regulated exploiting the geometry of the underlying surfaces which people believed to be a promising area capable of solving the problem of adhesion regulation. We have lucidly shown the potential of geometry in resolving excess or lack of adhesion issues through designing the required Gaussian Curvature of their substrates at the time of fabrication.

Scientists at NASA and other space agencies like European Space agency and SpaceX are showing their interest towards soft-robotics. Not just that, but many bio-robots are also being developed across the world for medical treatment techniques. The reason behind this is, such robots can minimize the damage cost by a huge amount, these are lightweight, so it can improve payload capacities in space missions. They can help doctors reach inner body harmlessly and treat humans and animals effectively. Soft-robots are made up of soft-elastic organic materials, at the microscopic scale they would also suffer from problems related to adhesive and frictional forces. In such a case, our work might help in enhancing the efficiency of such robots.

Our system consists of a rigid thin film on a soft curved surface which appears fre-

quently in nature e.g. fruits skin, animal skin, etc. This study may help understand their dynamics as well, open doors to new research strategies. So, to get a deeper understanding on the root of the problem and to be able to catch the missing link which can describe the effect that we observed in our experiments, we need to start from the birth of the theory of elasticity.

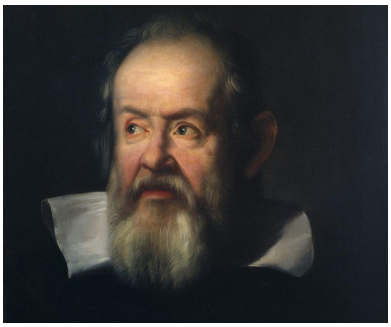

(a)

(b)

Fig. 1.1: (a) Galileo Galilei (1564-1642). Oil painting after Justus Wellcome Library, London. (b) Augustin-Louis, Baron Cauchy around 1840. Lithography by Zéphirin Belliard after a painting by Jean Roller.

Theory of elasticity is one of the famous theories in Physics. It has such an interesting spectrum of problems that this theory enthralled even the great minds of the past including Galileo, Euler, the Bernoullis, and others[5]. For the first time, the problem of Elastica was posed by Jordanus de Nemore in De Ratione Ponderis, which stated that "When the middle of a rod is held fast, the end parts are more easily curved", it was centuries after which it was explained with mathematical concepts. Then in 1638, Galileo raised a fundamental problem which asked how much weight is required to break a beam with its one end attached to the wall. He too proposed some solution to it. Many others elaborated Galileo's work. Then in 1678, Hooke published his linear law of forces and deformation which stated "The Power of any Spring is in the same proportion with the Tension thereof... Now as the Theory is very short, so the way of trying it is very easie.". On this budding theory, James Bernoulli posed a more precise problem of rectangular Elastica in 1691, which he partially solved as well in 1692 and published his first solution in 1694.

The development of the general 3-Dimensional theory of elasticity took place in the early 1820s with Cauchy's work on stress tensor[5]. Later, August Foppl and Theodore von Karman gave a set of nonlinear partial differential equations describing large deflections of 2-D sheets in 1907 and 1910 [6]. Those equations were derived by solving for equations of motion from Euler-Lagrange equations. Their theory describes how to calculate total stretching energy and total bending energy across the thickness of the sheet. But it doesn't describe the out-of-plane bending deformation energy. This computation of out of plane deformation is tough because of its non-linearity, computational require-

ments and unavailability of techniques to measure deformations without disturbing the processes accurately. Hence, people, these days are working on developing ways to calculate energies for out-of-plane deformations. And the effect that we observed in our experiment is a result of both stretching and out-of-plane bending of a 2D sheet. So, the study of out-of-plane deformation was the missing piece in the history of elasticity which can account for the dependence of solid to solid friction on a geometrical parameter. Because our experiment shows that in this small length scale, this dependence is notable. Therefore, it is necessary that we understand how friction scales with the geometry of the underlying surface.

1.1 Motivation for this experiment

While working on crumpling, we are trying to study the effects of elastic energy, this might help us back-calculate out-of-plane bending energy. When we talk about the microscopic world, the forces that we don't even realize in day to day life become significant in various phenomena that one observes. It is because all the forces have some range of length scale where it dominates over other forces. Since our experiment ranges in few hundred nano-meter thicknesses, forces like adhesion, friction and mechanical forces dominate over other kinds of forces. In this regime, these forces can be regulated largely by tweaking parameters by small values. One such parameter that we found is surface geometry which can regulate elastic stress, adhesive and frictional forces notably.

To realize this dependence on surface geometry, let's first understand how friction and adhesion are defined.

1.1.0.0 Friction

Friction is the result of electromagnetic interaction between surfaces. There are mainly two types of friction:

1. **Static friction :** It acts between surfaces which are not moving relative to each other.
2. **Dynamic/kinetic friction :** It acts between surfaces which are moving relative to each other.

Three empirical laws describe the behaviour of solid to solid frictional interaction:

1. **Amonton's First Law :** It says that frictional force is directly proportional to the applied load.

2. **Amonton's Second Law:** It says that friction is independent of the apparent area of contact.

3. **Coulomb's Law of Friction:** It says that kinetic friction is independent of sliding velocity.

It is important to note that the solid-solid frictional interaction is proportional to the applied load. So, the total vector sum of the loading force will determine how much friction does an object experiences.

1.1.0.0 Adhesion

Particles tend to attract particle of another kind. It arises because of intermolecular forces. It can cause an increase in frictional interaction by increasing the loading force. The two different objects involved here can exist in different phases as well. The possible combinations of states where adhesion can arise are:

1. **Solid to solid adhesion**

2. **Solid to liquid adhesion**

3. **Liquid to liquid adhesion**

Adhesion energy is measured in terms of Surface energy. Surface energy is the free energy change γ when the surface area of a medium is increased by unit area, which is equivalent to separating two half unit areas from contact[7].

$$\gamma_1 = \frac{W_{11}}{2} \tag{1.1}$$

Where γ is energy per unit area

The kind of adhesion involved in our experiment is shown below in Fig. 1.2 below

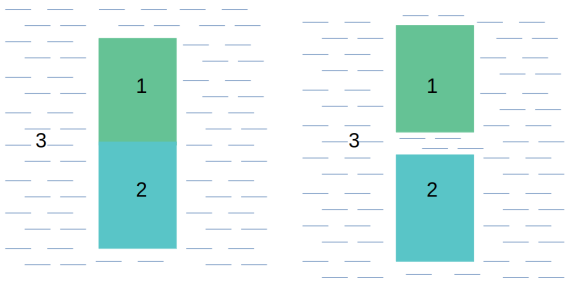

Fig. 1.2: This figure shows two solid blocks of different materials 1 and 2 attached to each other inside a liquid of the third kind of material 3. 1 and 2 are separated after which space gets occupied by the liquid 3.

Dupre equation, which gives the amount of work that has to be done for this process of separating two objects in a liquid medium as shown in Fig. 1.2 is given as :

$$W_{132} = W_{12} + W_{33} - W_{13} - W_{23} \tag{1.2}$$

Where, W_{132} is the total work done during the process, the total adhesion energy. First, to separate 1 and 2, the amount of work that has to be done is W_{12}. Amount of work that has to be done for each unit area of object 1 and 2 is $W_{12}/2$. Similarly, W_{33} amount of work has to be done to separate liquid of half unit area from each other on both sides of the objects. When the two half unit area of liquid 3 will combine with one unit area of object 1 and object 2, we will gain W_{13} and W_{23} amount of energy.

1.2 Outline of the experiment

In order to study the frictional interaction in a crumpling scenario of a thin film with a solid substrate, firstly, we need a probe which can compress the sheet isotropically at a given constant rate. We chose the decorative commercial Hydrogel balls for this purpose. Next, we required a set-up through which we can observe and store the ongoing process in images. As it is a transparent system, we designed a customized set-up whose entities are explained elaborately in Chapter 2.

To conduct experiments, we raise an ultra-thin circular Polystyrene film on top of a swollen spherical hydrogel substrate as shown in Fig.1.3. Then the substrate along with the film is kept outside the water on a stage where we can observe and record the process of crumpling. As the substrate shrinks due to evaporation of water, it isotropically compresses the film on top of it. The film gets some initial folds[8] which later evolve into a complex pattern consisting of wrinkles, folds and crumpled ridges. In the end,

we analyse the time-lapse of the whole process to study both the pattern as well as the frictional interaction between the ball and the film without disturbing the sheet while the experiment is going on.

(a) (b)

Fig. 1.3: Orange Film confined to the ball (a) before, (b) after. This image shows how our system looks before and after raising the film on the ball.

To analyse this complex system one needs to have precise control over many parameters like the thickness of the film, size of the film, adhesion between the film and the substrate, evaporation rate of the substrate, pattern distribution etc. While some aspect of this experiment is under development, we could experimentally realize the dependence of frictional interaction between the substrate and the film on substrates underlying Gaussian curvature. We could do this by examining the rate at which hydrogel and film are shrinking and getting compressed respectively from the images and if there is any correlation among them through image analysis.

While doing so, we also came across various interesting observation presented in Chapter 4 for future references.

There are a few useful reading materials for mechanics of deformations and image analysis which can be found here in the following references [9][10][11][12].
All the codes for image analysis can be found in the Appendix as well as in the following GitHub link, `https://github.com/zorawar12/MS-Thesis`

Chapter 2

Materials and method

In this chapter, we will look at each component of this experiment. How they are used and what was the purpose of using that apparatus. We will also see how this experiment was done in details including methods to prepare hydrogels and polystyrene films. Most importantly, we will see how to set up the contrast and background to image films on top of the ball and what is the convention of data arrangement in folders to be able to run the codes and reproduce the data and do analysis on them.

2.1 Hydrogel balls

A hydrogel is hydrophilic water gel which can absorb a very large volume of water compared to its dry state volume. Commercial ones are spherical in shape and are composed of a water-absorbing super-absorbent polymer (SAP, commonly known as slush powder in dry form)[13] such as polyacrylamide bound together with the help of a cross-linking molecule. And depending upon the type of polymer and the cross-linking molecule, the physical properties of the beads are determined. Commonly, these are used as decoration objects, for agricultural purposes, in sanitary napkins, etc. The commercially available dry beads range from 1-2.5mm in diameter. And when they completely swell, the diameter ob the ball ranges from 1.2-2.5cm. There are other larger size variants are also available in the market. In general, gels are considered as soft solid materials. The image of these balls and chemical is shown in Fig. 2.1.

(a)

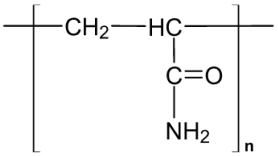

(b)

Fig. 2.1: (a)Hydrogel balls, (b) Polyacrylamide (Wikipedia), the building block of hydrogel balls

Hydrogel preparation procedure[14]:

1. Firstly, a pre-gel solution of the monomer N-(hydroxymethyl)-acrylamide (48% solution in water, Sigma-Aldrich) of the desired concentration is prepared in deionized water.

2. 0.25% of potassium persulfate (99.99% trace metals basis, Sigma-Aldrich) by weight and 0.3% of N, N, N, N-tetramethylethylenediamine (TEMED, $\geq$ 99.5%, purified by re-distillation, Sigma-Aldrich) by weight was then dissolved into the pre gel solution.

3. After mixing, within 10 minutes, the solution starts polymerizing. So before polymerization starts, the solution is kept in the mould of the desired shape.

Method to get hydrogel surfaces of various Gaussian curvatures:

1. **Spherical (Positive convex Gaussian surface):** They are commercially available in this shape. It can also be prepared in the above-described method with a spherical mould like a Table Tennis ball.

2. **Flat (Zero Gaussian surface):** It can be prepared using a flat mould or else the commercially available balls can be cut into hemispheres using a sharp blade and the flat part of the hemisphere can be used as a flat surface.

3. **Cylindrical (Zero Gaussian surface):** It can also be prepared using a cylindrical mould or else the top part of the commercially available balls can be cut by rotating the ball along the axis parallel to the blade and oscillating the blade from its edge to edge. The cylindrical part so obtained can be used. It often gets non-zero Gaussian curvature if not cut properly.

4. **Bowl (Concave positive Gaussian surface):** This can be prepared using a mould or else the commercially available balls can be cut into required shape using a sharp curved blade rotating along an axis like scooping an ice-cream and the generated surface is a desired one. This method of cutting often breaks the ball due to the curvature of the blade.

5. **Saddle (Negative Gaussian surface):** It can be prepared using a mould or else the commercially available balls can be cut using a sharp curved blade by scooping along with rotating the ball and the generated internal part of the ball can be used as a saddle surface. This method of cutting also breaks the ball very often.

2.2 Polystyrene films

Polystyrene[15] is a hydrophobic compound shown in Fig.2.2, commonly used as plastic material, for instance, Petri dishes are made using this. It is an aromatic hydrocarbon polymer made from the monomer styrene. They come in the form of beads of 2-3mm in diameter. We use these beads to prepare our ultra-thin films.

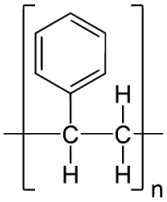

Fig. 2.2: Polystyrene (Wikipedia)

Method to prepare the ultra-thin films[16]:

1. Firstly, 0.02wt% Nile-Red solution is prepared by dissolving it in Toluene through a vortex mixer.

2. Then the required thickness in terms of wt% is decided, say 5wt%. And based on the weight of total solution that is required, 5% of the total weight is taken to be Polystyrene beads and the rest of the weight is filled with Toluene-Nile-red solution.

3. Then the mixture is well mixed through the vortex mixer. It is mixed until the Polystyrene dissolves in it completely.

4. The solution is then labelled and kept for a day to allow the polystyrene to dissolve homogeneously throughout.

5. After one day, clean glass slides are kept on Spin coat machine with say 1500RPM, for 1 minute with an acceleration of 3.

6. After that, Acetone solution is spread over the glass slide and the slide is cleaned by spinning it.

7. Wait for a minute to allow the slide to dry out, then the PS+Toluene+Nile-Red solution is homogeneously spread on top of the glass slide.

8. The slide is then spin-coated with the solution.

9. It is usually easy to cut-out the film one day after it is coated.

2.3 Imaging set-up

Below there is a schematic of the experimental set-up shown in Fig.2.3a. There are four major components to generate the kind of contrast required to be able to see the film of a few hundred nano-meter thick:

1. **Light obstructing disc :** This is used to not allow light to pass through the centre of the ball. This is required because these balls are transparent. It is kept right below the ball. And its diameter should be decreased with time. Image of this template is shown in Fig.2.3b

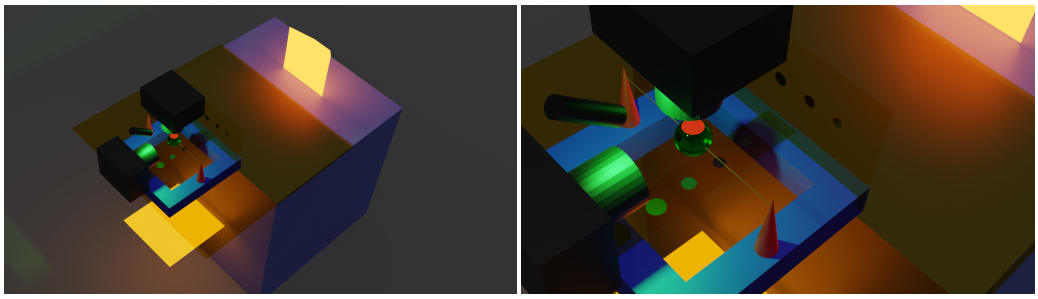

(a) (b)

Fig. 2.3: (a)Experimental set-up showing two white DC light sources, two cameras one at top and one at the side, a laser in between two cameras to fluoresce the film, (b) Closeup view of the ball hanging on thin wire supported by two crocodile clips with light obstructing disc right below it and film on top of the ball.

2. **Background light with diffuser :** This light source should be a DC light. Else the flickering of light will become noise for analysis. This light is used to see the boundary of the ball.

3. **Laser :** A laser light of wavelength 532nm is used to excite the fluorescence in the dye Nile red which is present in the film. The film fluoresces with an orange colour which creates the required contrast between the ball and the film. Thus making it easy to see the film as well as the patterns so formed on it.

4. **Camera and Low pass filters :** We used Nikon D5300 Camera with Micro Nikkor 60mm Nikon lens. It was equipped with three Low pass filters, to reduce the noise due to the laser used to excite the fluorescence. For imaging, we kept our camera in Manual mode, with Aperture size F40 to get wide-area under focus and different Exposure times ranging from 1/5" to 10" depending upon the generated contrast between the ball and the film due to different curvature and shapes of the substrate. For different experiments, we set different interval times for imaging to look at long time changes and short-time changes and this can be controlled through Laptop using a Python-Arduino integrated code or Arduino controlled IR blaster remote control if one needs images in different intervals in a single run. Both the codes are described in Appendix III and IV.

2.4 Useful handling tools and techniques

2.4.1 Ball raiser

This is a ring-shaped raiser with a slider to be able to change rings diameter to increase its range of applicability as shown in Fig.2.4a.

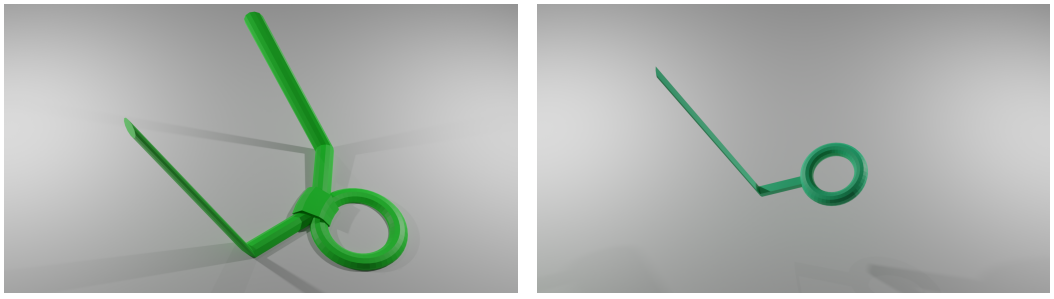

(a) (b)

Fig. 2.4: (a) Schematic of ball raiser : Ball is raised using the 'o' ring part whose diameter is adjustable, (b) Schematic of film raiser : Film is raised using the 'o' ring part using a liquid film like soap film.

2.4.2 Film raiser and holder

In this method, a water film is formed using the ring in Fig.2.4b similar to that of a soap film used to create soap bubbles. The ring is taken out of the liquid such that film is

encompassed by the periphery of the ring with faint air blown through the mouth on film to avoid film collapsing on the ring due to impulse created due to film formation, the film can be raised flat on water or soap film so formed.

Caution: It is more likely that the film will collapse due to impulse from film formation.

2.4.3 Film stamper

This method is used to transfer the film onto a ball cut out into a surface with the required curvature. In this method, the film is raised on a ball cut with another half of the desired Gaussian curvature. The film is then stamped on the required surface. This method is only useful if substrate gel has to be protected from getting water.

2.4.4 Hole maker and hydrogel cutter

A cylindrical hollow pipe of the desired diameter is used to make a hole on hydrogels. It should be pierced at once by holding the ball with a tissue paper. Sharp blades are used to cut hydrogels. Slow and steady oscillation is the best way to cut using blades.

2.4.5 Film shape template

This is used to cut film of desired shape and size. It is a mask template as shown in Fig.2.5.

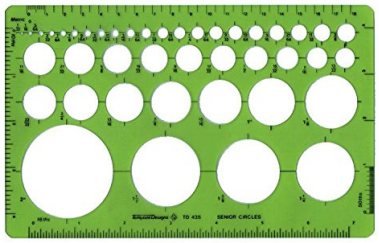

Fig. 2.5: Mask for cutting film. Image courtesy: www.amazon.in

2.4.6 Stage to mount the substrate with the film

This is one of the most important parts of this experiment, as an unstable stage can introduce lots of noise and unwanted camera effects, movement of the ball particularly during experiments run over long periods, etc. which cannot be resolved.

It is an 'O' shaped object with crocodile clips at its two ends placed on the same horizontal line. A thin capillary tube is used to pierce hole slightly(1mm) above the horizontal great circle of the ball. Then a thin wire of diameter less than 0.5mm is passed through the tube and the tube is then removed. The two ends of the wire are then tightly tied to the crocodile clips. The wire should be thin enough to not hinder in image analysis. A schematic 3D diagram of the stage is shown in Fig 2.6.

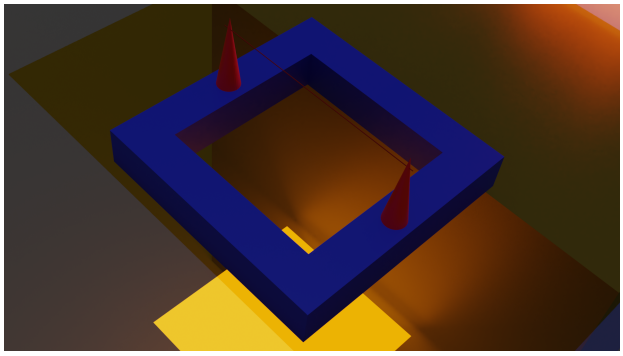

Fig. 2.6: Schematic of the stage, Red cone represents the crocodile clip and the ball is hanged on the red wire.

2.5 Camera and Laser control through Arduino

These experiments run over a period of many hours. Images are taken periodically at certain time intervals. To protect the laser from damages arising due to running continuously over many hours, we switch on the laser only during the period when the camera takes images. The image taking and the switching on of the laser light is synchronized using an Arduino board. For this, the camera is kept in Remote control mode with remote sensor timeout setting more than the imaging interval. The void takePhoto[17] part of the code sends a particular frequency packet of IR blast which is defined for this Nikon camera. Then the IR led gives the corresponding output whenever takePhoto() function is called. The code inside the void loop controls the laser connected to Pins 8

and 12. Time delays here has to be set for each experiment based on interval time and the exposure time. IR Led is kept close to the Camera IR sensor to avoid any cycle of imaging.
The circuit diagram of the controller is shown in Fig.2.7:

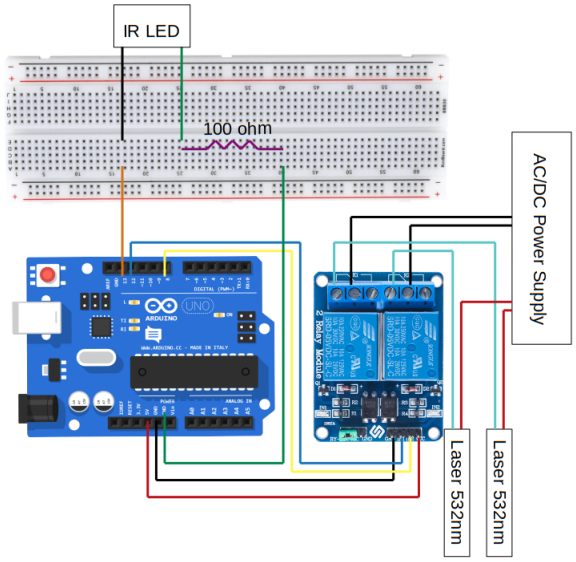

Fig. 2.7: Circuit diagram showing Arduino controlling Relays which act as a switch for the lasers, and the IR LED which remotely controls Cameras using IR radiation of specific frequency pulses.

For codes, refer to Appendix III.

2.6 Camera and Laser control through the laptop

The following Python code controls the camera through laptop. It is self-descriptive through comments in the code. For this code to work, all the libraries should be installed and the serial port must be up and running through the Arduino. The serial port name should be changed to the same as Arduino's. First Arduino code should be run and then python code. Throughout this entire process, images are being taken by an open-source software called qDslrDashboard_V3.5.9_Linux_x64 and stored in the same folder where python code is running. The same circuit shown in Fig.2.7 is used. For codes, refer to Appendix IV.

2.7 Procedure and analysis technique

This section gives a complete description of the steps followed and codes used to analyse the images acquired during this project.

Steps to reproduce the experimental results:

1. Polystyrene thin films are prepared by following the steps mentioned in section 2.2.
2. Hydrogel ball is swollen using Mili Q water to its largest size.
3. Polystyrene film of the desired shape, size and thickness is cut out from the prepared slides using the film shape template shown in Fig.2.5.
4. The film is then floated on top of Mili Q water surface in a bowl.
5. A thin capillary tube is pierced through the centre of the hydrogel ball.
6. The ball is then submerged in the bowl along with the capillary tube.
7. The ball along with the capillary tube is then raised using a ball raiser shown in Fig. 2.4a, such that the film gets confined on top of the ball.
8. One end of a thin wire of diameter less than a millimetre passing through the centre of a scaling button whose one end is already tied to the stage is pierced across the ball through the capillary tube.
9. The capillary tube is then removed from the ball once the wire is taken out on the other side and the other end of the wire is then tied tightly to the stage as shown in Fig. 2.3b.
10. The lighting is set for both top and side view such that film and the ball boundary are visible in the image using the black discs below the ball as shown in Fig. 2.3a.
11. Camera settings are done as explained in section 2.3. If controlling the system with Arduino, laser and camera both should be connected to the Arduino as explained in section 2.5. Else, both the camera's with the required time interval is set to take photographs.
12. If controlling camera and laser through the laptop, connect the camera through USB to the laptop. The folder named camlivecontrol has to be kept in Desktop. It contains a python code-named lasercontrol.py and an Arduino code-named Lasercontrol.ino. The python code and the Arduino code are explained in Appendix IV and III. Follow the steps explained in section 2.5 to start taking images.

Conventions of data arrangements and steps to analyse the timelapse of images obtained, few useful numerical techniques used can be found here[18][19][20]:

1. Folder of experiments is named as YYYYMMDD.

2. The hierarchy of directory is set as $Nilered/Curvature/ < Type\_of\_curvature > / < Thickness\_in\_wtper > / < film\_to\_ball\_initial\_radius\_ratios > / < film\_size\_in\_mili\_inches > /YYYYMMDD/$.

3. Each YYYYMMDD folder contains 'topview' folder, 'sideview' folder and a Lasercam folder. The Lasercam folder contains Arduino code to control the camera and laser both together using a relay module and IR blaster as explained in Appendix IV and III.

4. Each 'topview' and 'sideview' folder contains raw images from the camera, an experiment description.txt file, a folder named dynamics and time.m file.
   NOTE: Only images to be analyzed should be kept here, extra images should be dumped inside dynamics folder.

5. The description.txt file should contain all experimental parameters chosen for that particular experiment like film size and thickness, etc. The time.m file when run, gives two files as output inside dynamics folder named as time.ods and timestamps.ods.

6. The dynamics folder contains cropped .tif images of the images that have to be analyzed, an analysis.m file and a regionellipse.m file or a sideview.m file and a sideanalysis.m and a folder named cropped which will contain all the cropped images for film and ball and the binary images for the film and the ball separately.

7. The outputs of all the codes are saved inside the folders named 'anaN' inside the dataN(N = number) inside the cropped folder.

   NOTE: All the codes are available and explained individually with comments in the Github link provided here 1.2 and also in Appendix V.

8. To do the analysis first time.m should be run, then the regionellipse.m or sideview.m files should be run, after those programs give output, the analysis.m or sideanalysis.m files should be run. This will provide the plots for deriving inferences of this experiment.

2.8 Film thickness measurement

The thickness of the film was measured using the J.A. Wollam Ellipsometry device. It uses an elliptically polarized light to calculate the thickness of the film by measuring the change in polarization of the light after reflection from the surface of the film loaded on top of UV-Ozone cleaned N-type silicon wafers. The thickness of the films used in our experiments is listed below in Table.2.1

Tab. 2.1: Film thickness measured through Ellipsometry

Film_name(in wt%)	**Dye**	**Solution_name**	**Thickness(in nm)**
Blank Silicon	_	_	250
1	Nile-Red	Solution_4	60
1	Nile-Red	Solution_2	60
2	Nile-Red	Solution_3	149
4	Nile-Red	Solution_4	321
5	Nile-Red	Solution_4	467
5	Nile-Red	Solution_1	426
1	_	Solution_0	72
2	_	Solution_0	144
2(Nitin's)	_	_	245
15	_	Solution_0	1403

Chapter 3

Results

This chapter describes the important results which show the variation of rate of compression of a film with the underlying Gaussian curvature of the substrate. First, we have shown how the ball and film look like in a typical image data, followed by this, we have shown our conventions for image analysis in both top and side views and what is in the image that we call as patterns. Then we describe the importance of side-view imaging. In the end, we show that data which leads us to our conclusion and it is then supported with confirmatory experiments.

3.1 Introduction to typical raw image and conventions

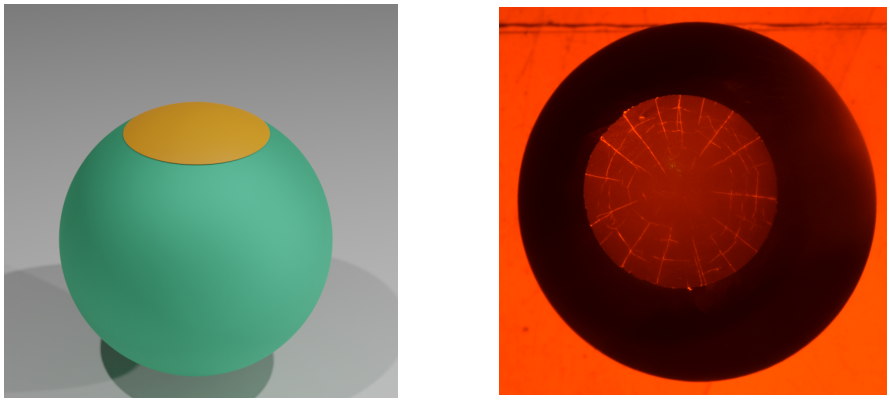

(a) (b)

Fig. 3.1: (a) 3D schematic of the film on the ball, (b) Actual image of the film on top of the ball after 2 hours of initiation

3.1.1 Top view

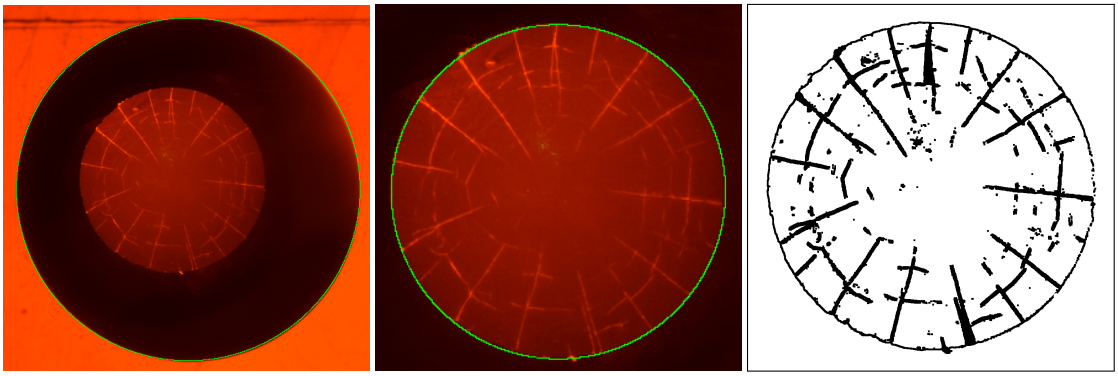

(a) (b) (c)

Fig. 3.2: Top view image: (a) Ball boundary in green colour detected through code(R), (b) Film boundary in green colour detected through code(r), (c) Processed image showing detected pattern

To detect the ball boundary, We binarize the raw image, then remove noise outside the certain boundary and fill the holes of the inverted image, then operate the open operation in binary with iteration set to 2-5 in the ImageJ software. We use this image to detect the ball boundary using regionprops[20] or imfindcircle[19] in MATLAB. Similarly, we detect the film boundary using films binary form as shown above in Fig.3.2. Detailed processing is explained in the codes.

3.1.2 Side view

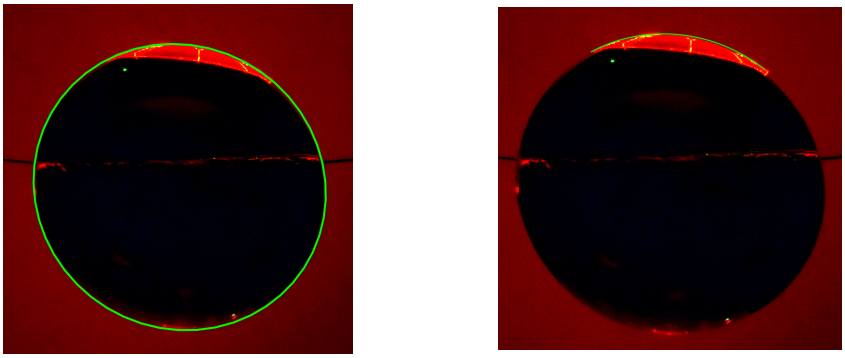

(a) (b)

Fig. 3.3: Side view image: (a) Ball boundary in green colour detected through code(R), (b) Film boundary in green colour detected through code(W)

To detect the ball boundary, We binarize the raw image, then remove noise outside the certain boundary and fill the holes of the inverted image, then operate the open operation in binary with iteration set to 2-5 in the ImageJ software. We use this image to detect the ball boundary using regionprops[20] or imfindcircle[19] in MATLAB. For the film, we take the grey image of the raw image and then scan all the rows for columns once from left and once from right to detect initial and final point of the film by setting some threshold as shown in Fig.3.3. And then we measure the film radius mathematically using the polar form of ellipse[21].

In both the views we use Major axis of the detected elliptical boundary and use circular approximations to find ball and film radius using major-axis as the radius of the circle to avoid complexities.

3.2 Why side view

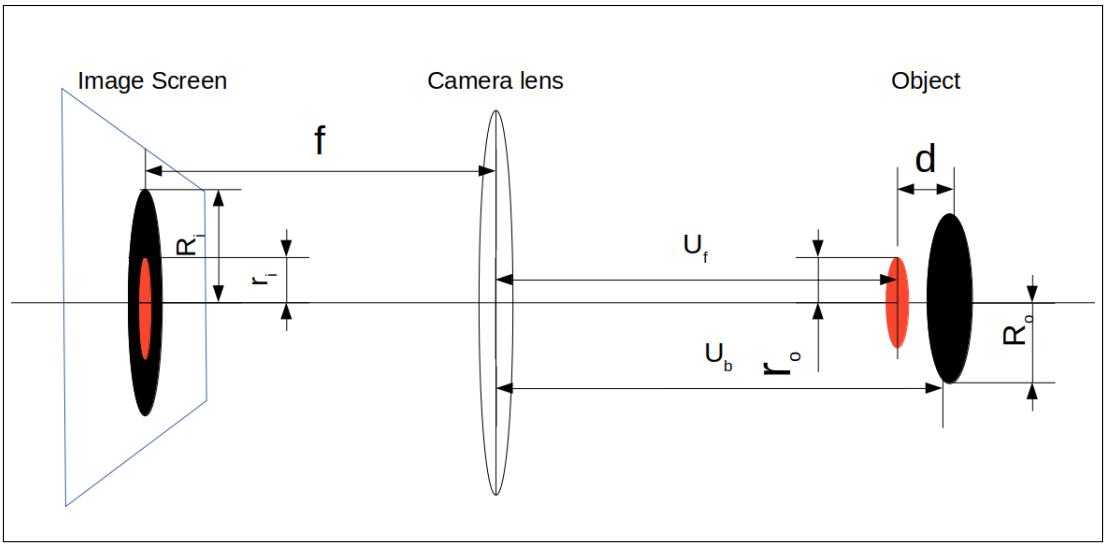

Fig. 3.4: Schematic ray diagram of top view imaging. The orange circle is the film and the black circle is the ball's central plane. Both film and ball are being measured at different distances from the camera but the image plane is the same for both.

Magnification formula from geometrical optics is given by

$$m = \frac{Image\ length}{Object\ length} = \frac{Image\ distance}{Object\ distance} \tag{3.1}$$

So, from Fig.3.4, image lengths of objects are given by

$$R_i(t) = mR_o(t) = \frac{R_o(t)f}{U_b(t)} \tag{3.2}$$

$$r_i(t) = r_o(t)m = \frac{r_o(t)f}{U_f(t)} \tag{3.3}$$

Normalized ball radius is given by

$$\frac{R_i(t)}{R_i(0)} = \frac{R_o(t)U_b(0)}{R_o(0)U_b(t)} \tag{3.4}$$

Since, we are looking at the top view of the object, in the image we see the projected radius of the film, so to get the actual radius of the film, we need to compensate for the curvature as shown in Fig 3.5.

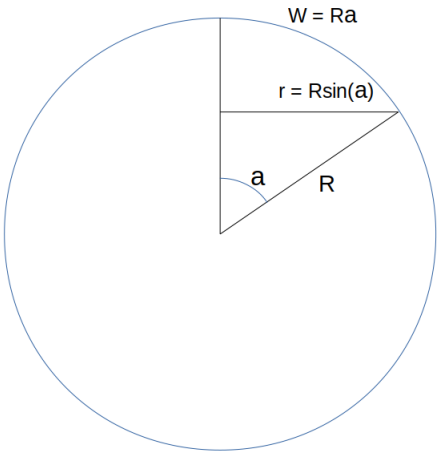

Fig. 3.5: The schematic diagram for compensation of films radius using projected radius 'r' of the film on a ball of radius R.

So, the compensated film radius is given by

$$W = Rsin^{-1}(\frac{r}{R}) \tag{3.5}$$

Now, in image length scale, compensated film radius (the one that we are calculating while analysing) is given by

$$W_i(t) = R_i(t)sin^{-1}(\frac{r_i(t)}{R_i(t)}) \tag{3.6}$$

Normalized film radius is given by

$$\frac{W_i(t)}{W_i(0)} = \frac{R_i(t)}{R_i(0)}\frac{sin^{-1}(\frac{r_i(t)}{R_i(t)})}{sin^{-1}(\frac{r_i(0)}{R_i(0)})} \tag{3.7}$$

Substituting equation 3.2, 3.3 and 3.4 in equation 3.7 we get,

$$\frac{W_i(t)}{W_i(0)} = \frac{R_o(t)U_b(0)}{R_o(0)U_b(t)} \frac{sin^{-1}(\frac{r_o(t)U_b(t)}{R_o(t)U_f(t)})}{sin^{-1}(\frac{r_o(0)U_b(0)}{R_o(0)U_f(0)})} \tag{3.8}$$

Now the normalized ball and film radius at time (t+1) is given by equation 3.9 and 3.11 respectively.

$$\frac{R_o(t+1)}{R_o(0)} = \frac{R_o(t) - \Delta}{R_o(0)} \tag{3.9}$$

$$\implies \frac{R_i(t+1)}{R_i(0)} = \frac{U_b(0)}{U_b(t+1)} \frac{R_o(t) - \Delta}{R_o(0)} \tag{3.10}$$

$$\frac{W_o(t+1)}{W_o(0)} = \frac{W_o(t) - \mu W_o(t)\frac{\Delta}{R_o(t)}}{W_o(0)} = \frac{R_o(t)}{R_o(0)} \frac{sin^{-1}(\frac{r_o(t)}{R_o(t)})}{sin^{-1}(\frac{r_o(0)}{R_o(0)})}(1 - \frac{\mu\Delta}{R_o(t)}) \tag{3.11}$$

$$\begin{aligned} \implies \frac{W_i(t+1)U_b(t+1)}{W_i(0)U_b(0)} \frac{sin^{-1}(\frac{r_o(t+1)}{R_o(t+1)})}{sin^{-1}(\frac{r_o(0)}{R_o(0)})} \frac{sin^{-1}(\frac{r_o(0)U_b(0)}{R_o(0)U_f(0)})}{sin^{-1}(\frac{r_o(t+1)U_b(t+1)}{R_o(t+1)U_f(t+1)})} \\ = \frac{R_o(t)}{R_o(0)} \frac{sin^{-1}(\frac{r_o(t)}{R_o(t)})}{sin^{-1}(\frac{r_o(0)}{R_o(0)})}(1 - \frac{\mu\Delta}{R_o(t)}) \end{aligned} \tag{3.12}$$

$$\begin{aligned} \implies \frac{W_i(t+1)}{W_i(0)} = \frac{sin^{-1}(\frac{r_o(t+1)U_b(t+1)}{R_o(t+1)U_f(t+1)})}{sin^{-1}(\frac{r_o(0)U_b(0)}{R_o(0)U_f(0)})} \\ \frac{U_b(0)}{U_b(t+1)} \frac{R_o(t)}{R_o(0)} \frac{sin^{-1}(\frac{r_o(t)}{R_o(t)})}{sin^{-1}(\frac{r_o(t+1)}{R_o(t+1)})}(1 - \frac{\mu\Delta}{R_o(t)}) \end{aligned} \tag{3.13}$$

Where, $\mu = 0$ if the film is slipping and 1 if the film is completely stuck
Δ is the change in balls radius, depends on the rate of evaporation

So, the change at any time is given by

$$\frac{R_i(t+1) - R_i(t)}{R_i(0)} = \frac{U_b(0)}{U_b(t+1)} \frac{R_o(t) - \Delta}{R_o(0)} - \frac{R_o(t)U_b(0)}{R_o(0)U_b(t)} \tag{3.14}$$

$$\begin{aligned} \implies \frac{W_i(t+1) - W_i(t)}{W_i(0)} = \frac{sin^{-1}(\frac{r_o(t+1)U_b(t+1)}{R_o(t+1)U_f(t+1)})}{sin^{-1}(\frac{r_o(0)U_b(0)}{R_o(0)U_f(0)})} \frac{U_b(0)}{U_b(t+1)} \frac{R_o(t)}{R_o(0)} \frac{sin^{-1}(\frac{r_o(t)}{R_o(t)})}{sin^{-1}(\frac{r_o(t+1)}{R_o(t+1)})}(1 - \frac{\mu\Delta}{R_o(t)}) \\ - \frac{R_o(t)U_b(0)}{R_o(0)U_b(t)} \frac{sin^{-1}(\frac{r_o(t)U_b(t)}{R_o(t)U_f(t)})}{sin^{-1}(\frac{r_o(0)U_b(0)}{R_o(0)U_f(0)})} \end{aligned} \tag{3.15}$$

In completely stuck case, $\frac{r_o(t+1)}{R_o(t+1)} = \frac{r_o(t)}{R_o(t)}$. So, value of slope = (eq. 3.15/eq. 3.14) will be 1 if U's are ignored. But when we are looking at top view, with time film and ball's

great circle are coming closer and along with that both ball and film are moving away from camera, so $\frac{U_f(t+1)}{U_b(t+1)} > \frac{U_f(t)}{U_b(t)}$, $U_f(t+1) > U_f(t)$ and $U_b(t+1) > U_b(t)$, hence leading to slope greater than 1.

So, to resolve this, if we fix the ball's distance from the camera by hanging the ball through a wire passing through the centre of the ball and then taking images from the side so that $U_f(t) = U_b(t) = U_b(0)$.
So, the ratio now becomes

$$\frac{\frac{W_i(t+1)-W_i(t)}{W_i(0)}}{\frac{R_i(t+1)-R_i(t)}{R_i(0)}} = \mu \tag{3.16}$$

Now the maximum value that the slope can reach is 1. When the slope is 0, that means the film is slipping and when it is greater than 0, it means the film is sticking to the substrate but not completely. And the strength of adhesion is determined by the value of the slope. The larger the slope, larger is the friction due to increased adhesion.

3.3 Dependence of friction on Gaussian curvature

3.3.1 Convex positive Gaussian curvature

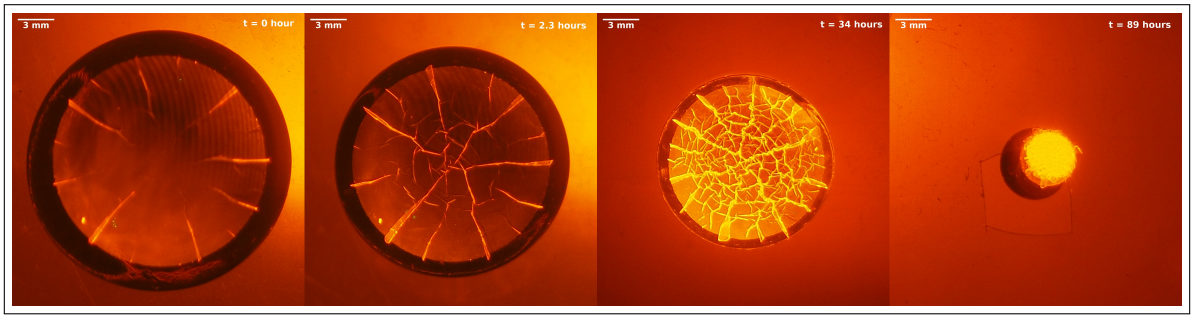

Fig. 3.6: The sequence of images from a full-length experiment on a substrate of convex positive Gaussian curvature.

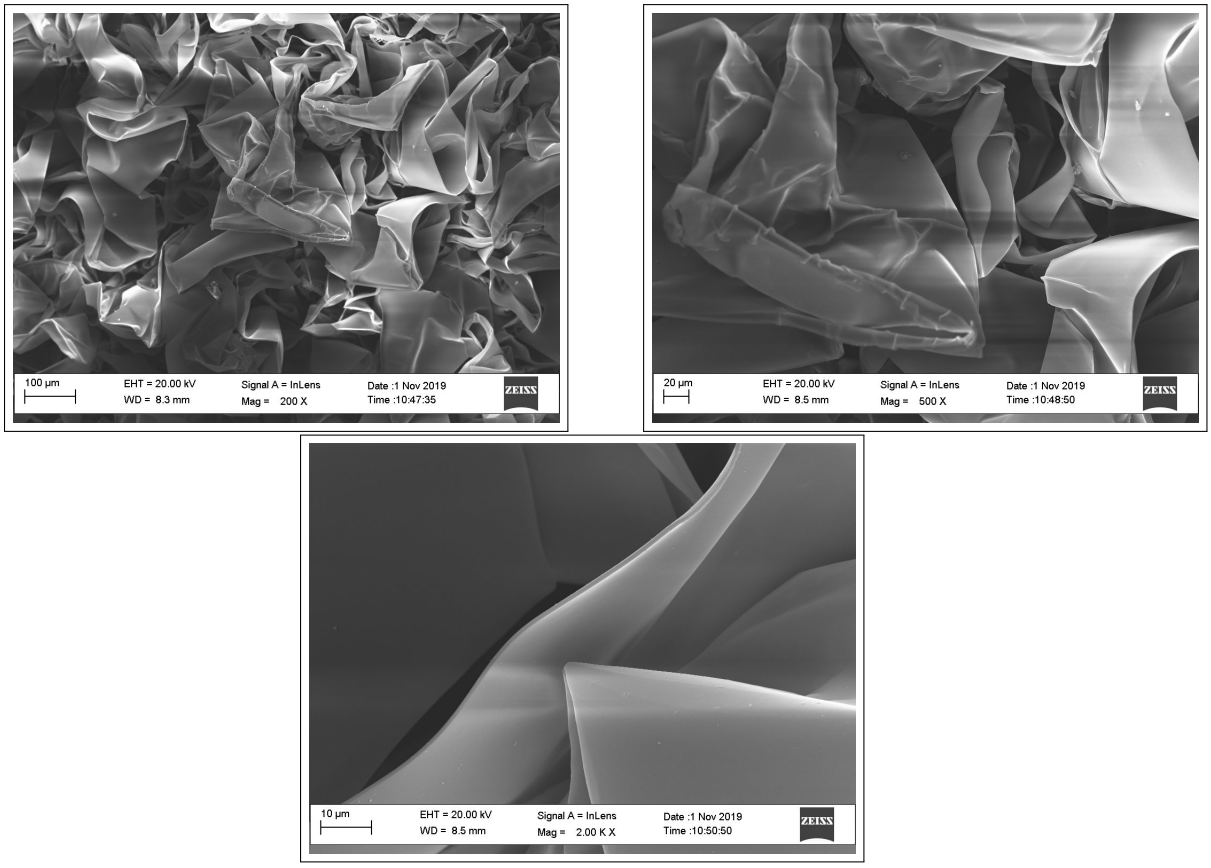

Fig. 3.7: Scanning Electron Microscope imaging of film in the final crumpled stage of the experiment taken at three different magnification.

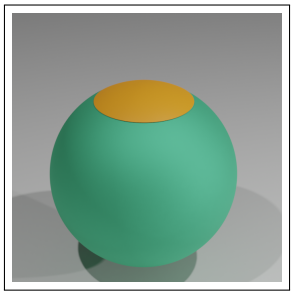

Fig. 3.8: Schematic of a film on a substrate of positive convex Gaussian curvature.

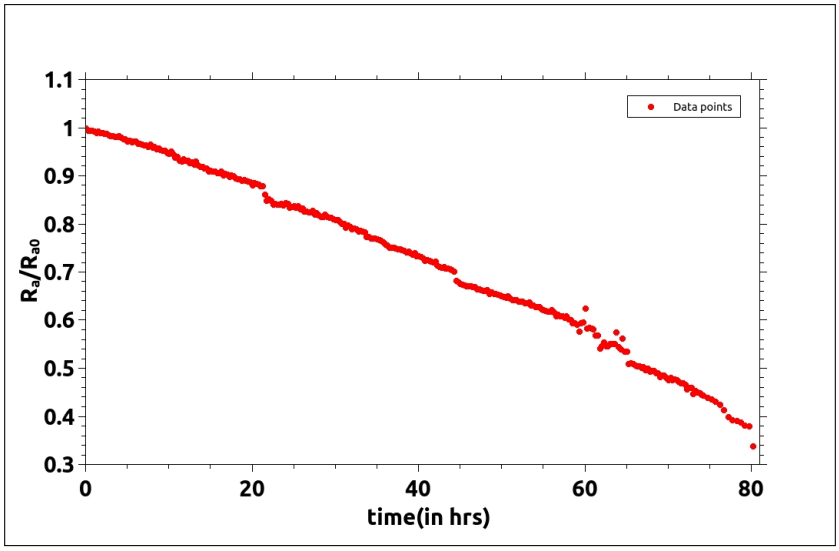

Fig. 3.9: Plot showing the time evolution of the major-axis of the ball.

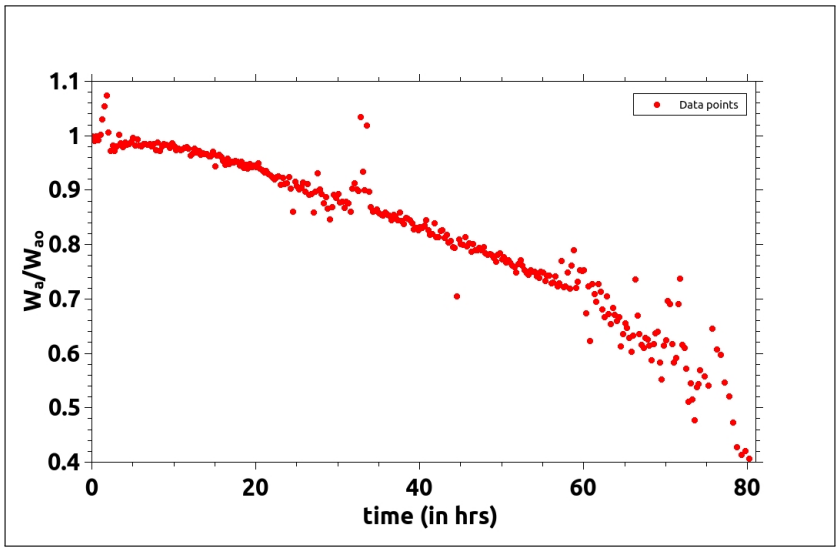

Fig. 3.10: Plot showing the time evolution of the major-axis of the film.

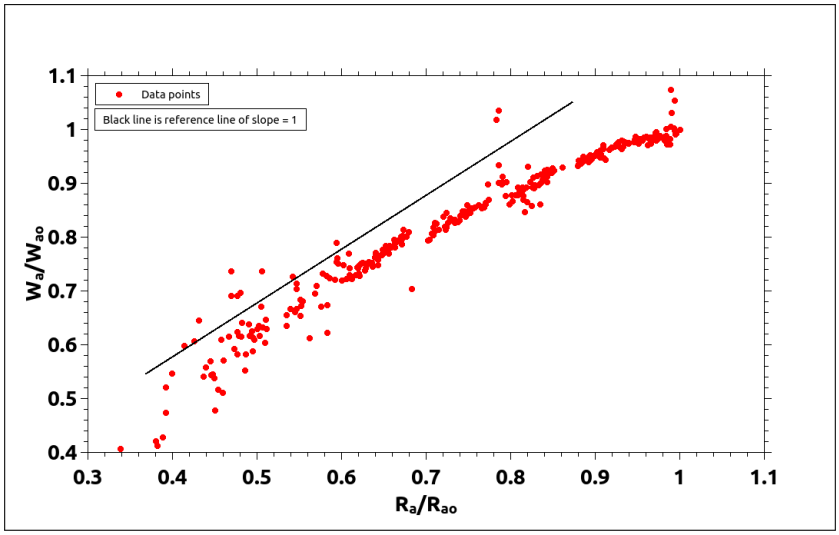

Fig. 3.11: Plot showing evolution of the major-axis of the film with respect to the major-axis of the ball.

Tab. 3.1: Experimental parameters for Fig. 3.11

Expt_Name	Film_ diameter (W_{a0})(in inches)	Film_ thickness (in nm)	Initial_ Ratio (W_{a0}/R_{a0})	Overall Slope	Hours of expt (in hours)
20191021	0.812	426	0.94	0.72	80

Here as the time progresses, the rate at which film size is reducing increases with respect to the ball. This is inferred from the slope in Fig. 3.11 which increases from 0 to 1 when moving from 1 towards 0 along x-axis. Throughout this whole experiment, the thickness of the film, size of the film, material of the ball and the film and hence the adhesion between the ball and the film due to their material property remains same but the only parameter that changes is the Gaussian curvature of the ball. Hence, giving a hint that rate of compression depending on Gaussian curvature of the substrate. So we conducted the following experiments on substrates of different Gaussian curvatures.

3.3.2 Convex positive Gaussian curvature

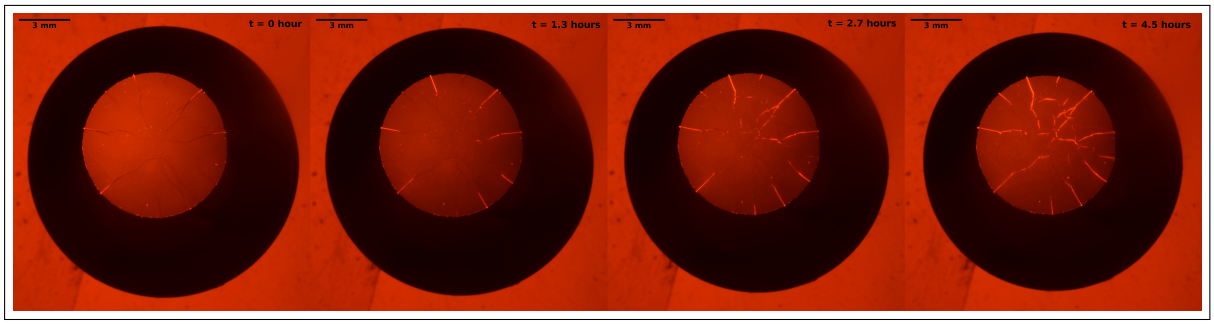

Fig. 3.12: The sequence of images from the experiment on the substrate of convex positive Gaussian curvature.

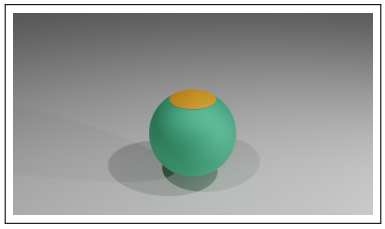

Fig. 3.13: Schematic of a film on a substrate of positive convex Gaussian curvature.

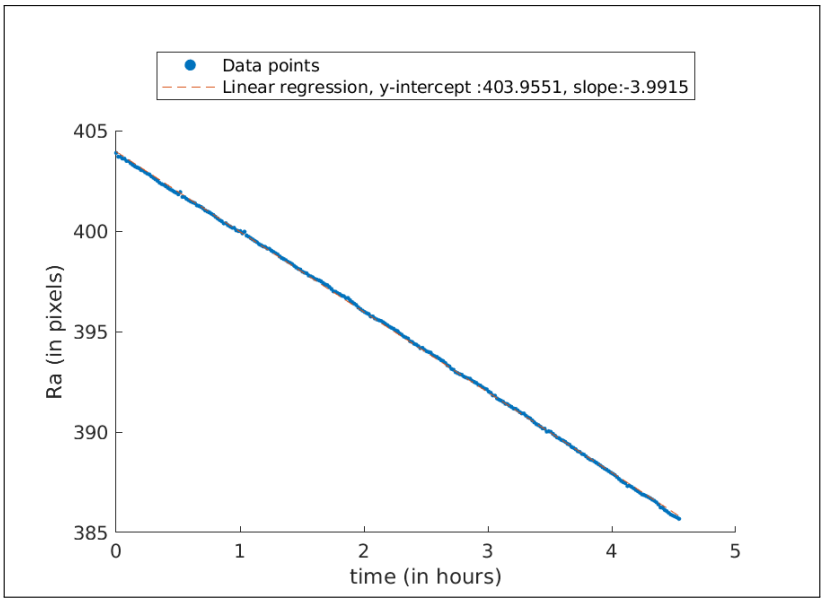

Fig. 3.14: Plot showing the time evolution of the major-axis of the ball.

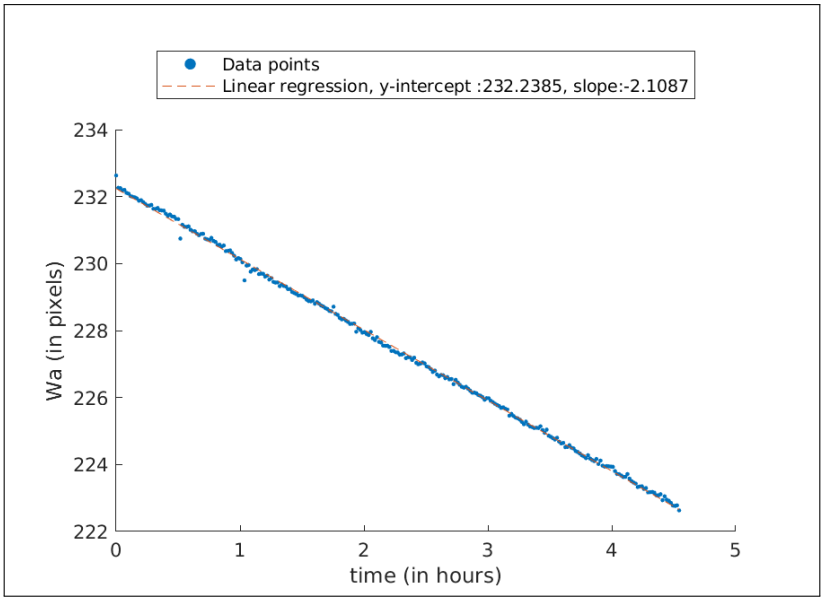

Fig. 3.15: Plot showing the time evolution of the major-axis of the film.

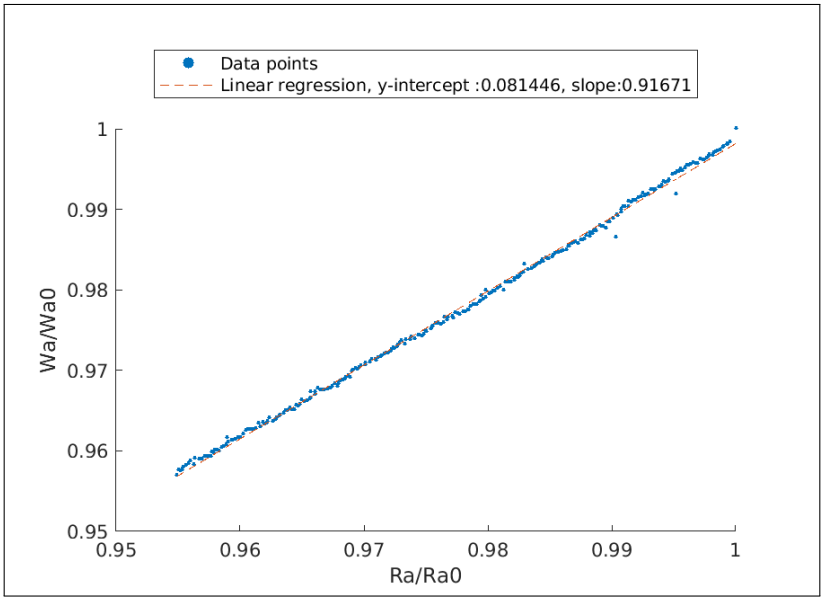

Fig. 3.16: Plot showing evolution of film major-axis with respect to the ball major-axis.

Tab. 3.2: Experimental parameters for Fig. 3.16

Expt_Name	Film_ diameter (W_{a0})(in inches)	Film_ thickness (in nm)	Initial_ Ratio (W_{a0}/R_{a0})	Overall Slope	Hours of expt (in hours)
20191221	0.328	467	0.54	0.91	4.54

3.3.3 Flat zero Gaussian curvature

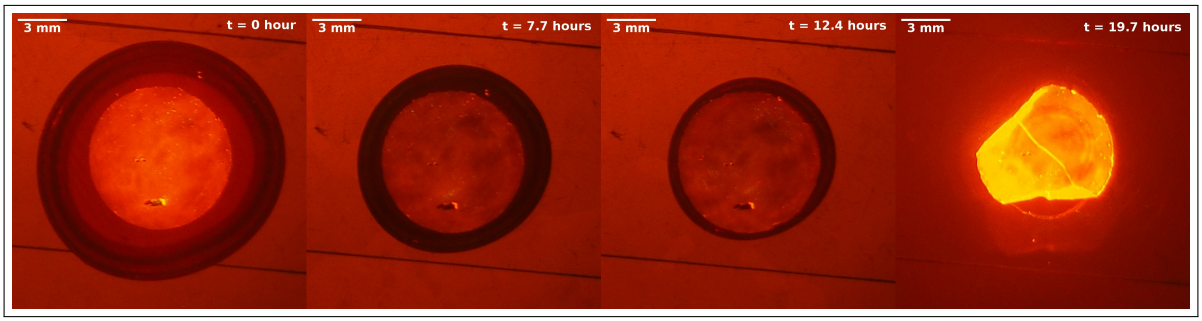

Fig. 3.17: The sequence of images from the experiment on the substrate of flat zero Gaussian curvature.

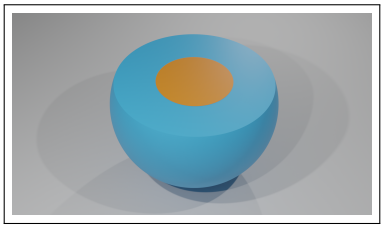

Fig. 3.18: Schematic of a film on a substrate of flat zero Gaussian curvature.

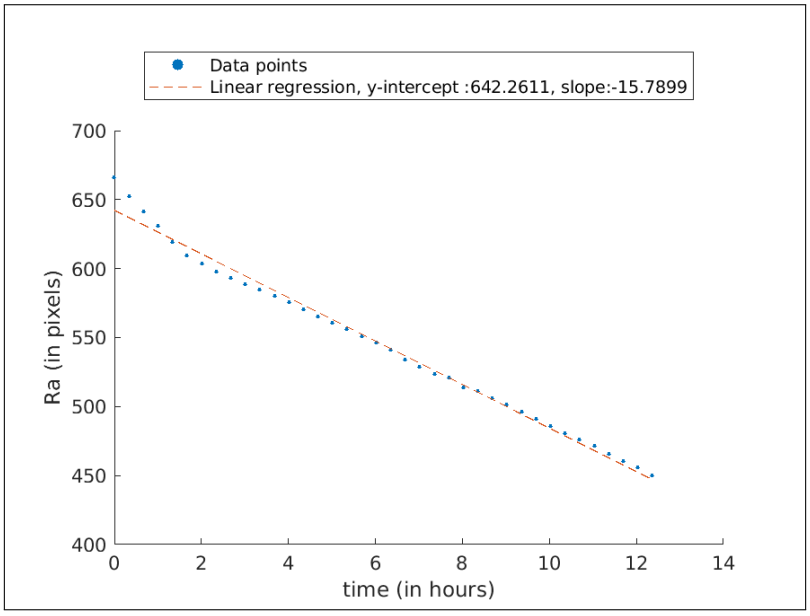

Fig. 3.19: Plot showing the time evolution of the major-axis of the ball.

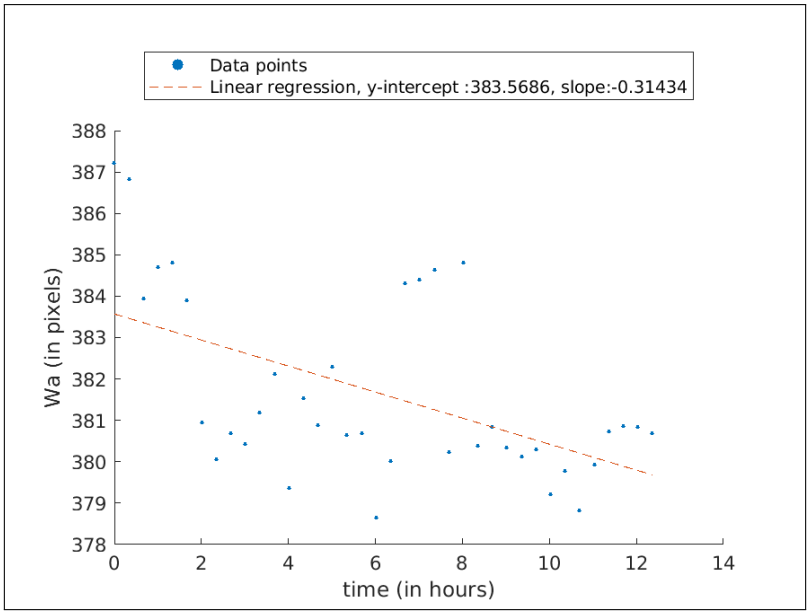

Fig. 3.20: Plot showing the time evolution of the major-axis of the film.

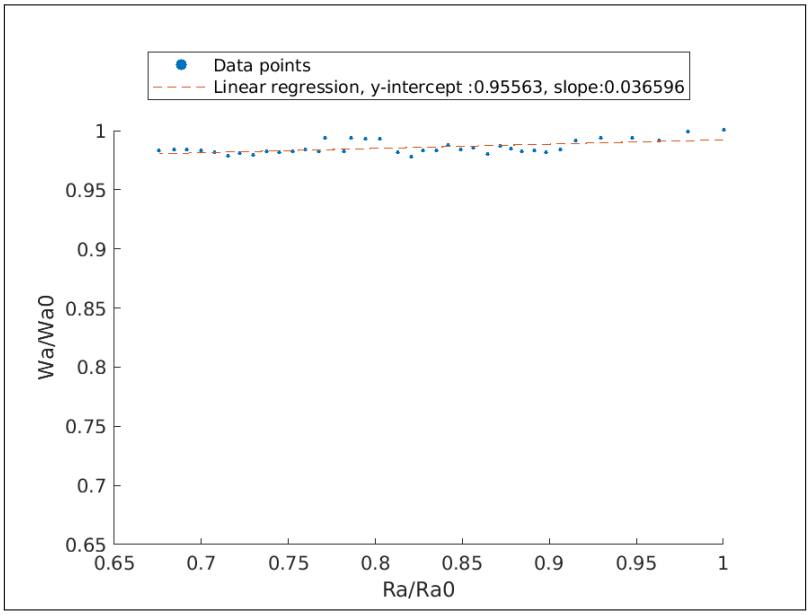

Fig. 3.21: Plot showing evolution of the major-axis of the film with respect to the major-axis of the ball.

Tab. 3.3: Experimental parameter for Fig. 3.21

Expt_Name	Film_ diameter (W_{a0})(in inches)	Film_ thickness (in nm)	Initial_ Ratio (W_{a0}/R_{a0})	Overall Slope	Hours of expt (in hours)
20191104	0.328	426	0.58	0.03	12.3

3.3.4 Cylindrical zero Gaussian curvature

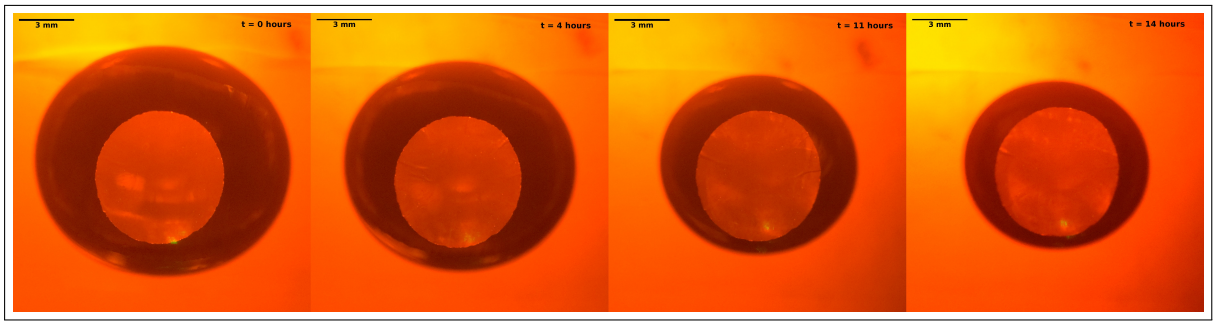

Fig. 3.22: The sequence of images from the experiment on the substrate of cylindrical zero Gaussian curvature.

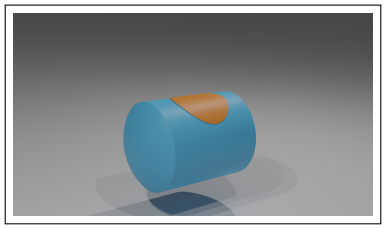

Fig. 3.23: Schematic of a film on a substrate of cylindrical zero Gaussian curvature

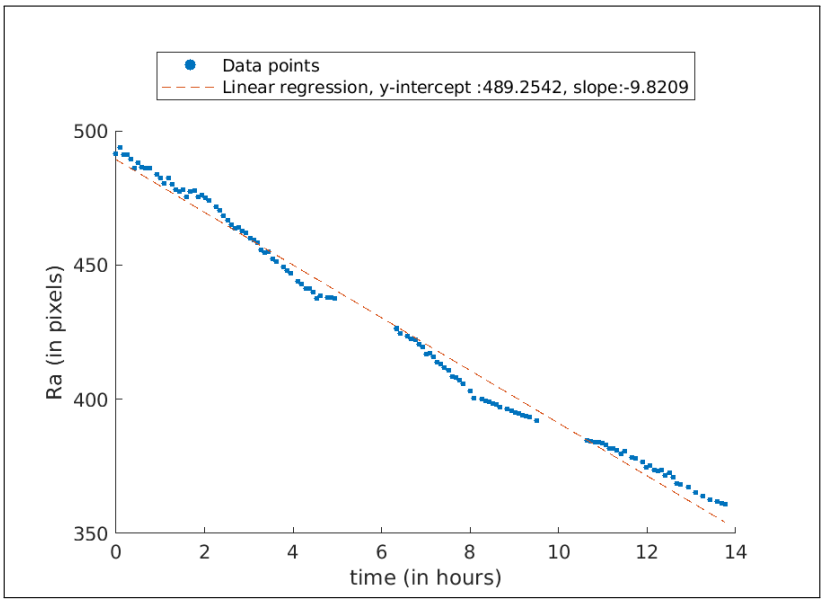

Fig. 3.24: Plot showing the time evolution of the major-axis of the ball.

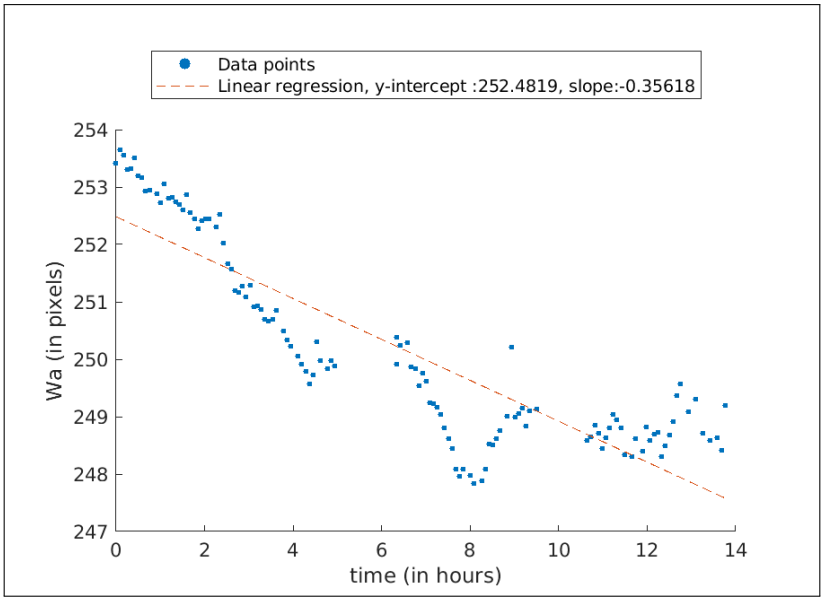

Fig. 3.25: Plot showing the time evolution of the major-axis of the film.

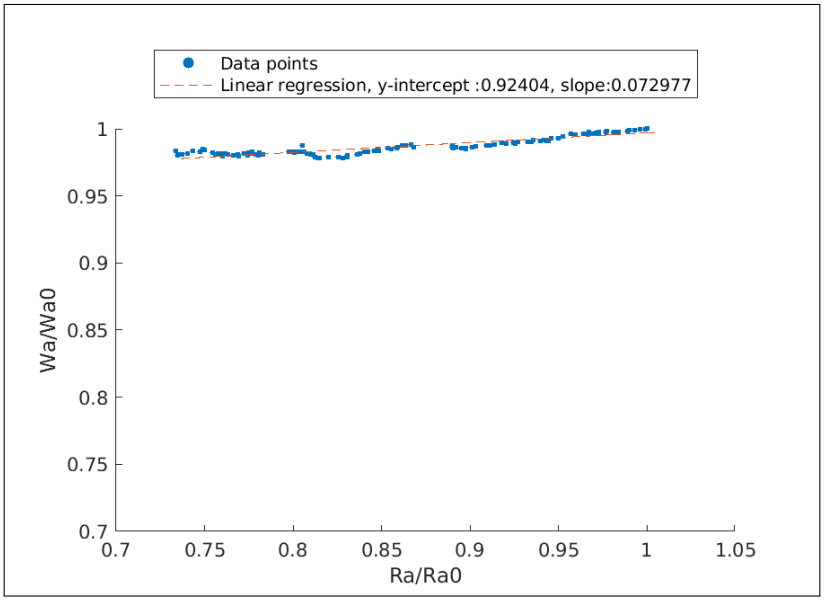

Fig. 3.26: Plot showing evolution of the major-axis of the film with respect to the major-axis of the ball.

Tab. 3.4: Experimental parameters for Fig. 3.26

Expt_Name	Film_ diameter (W_{a0})(in inches)	Film_ thickness (in nm)	Initial_ Ratio (W_{a0}/R_{a0})	Overall Slope	Hours of expt (in hours)
20191204	0.328	426	0.51	0.07	13.76

3.3.5 Concave positive Gaussian curvature

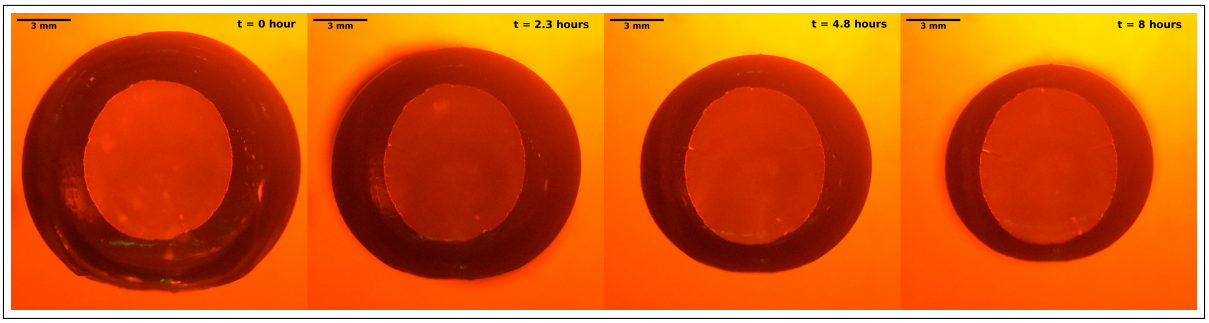

Fig. 3.27: The sequence of images from the experiment on the substrate of concave positive Gaussian curvature.

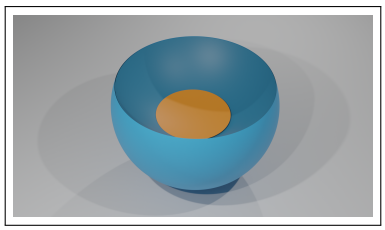

Fig. 3.28: Schematic of a film on a substrate of concave positive Gaussian curvature

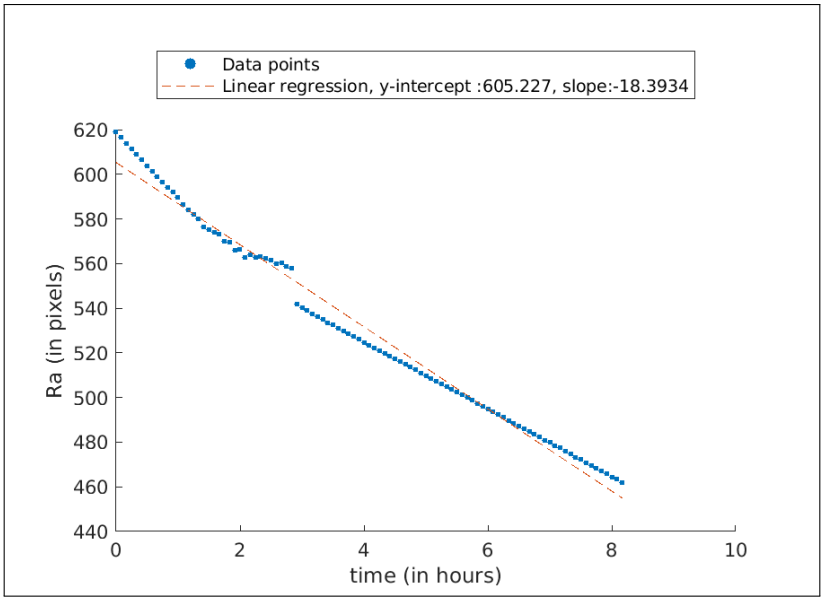

Fig. 3.29: Plot showing the time evolution of the major-axis of the ball.

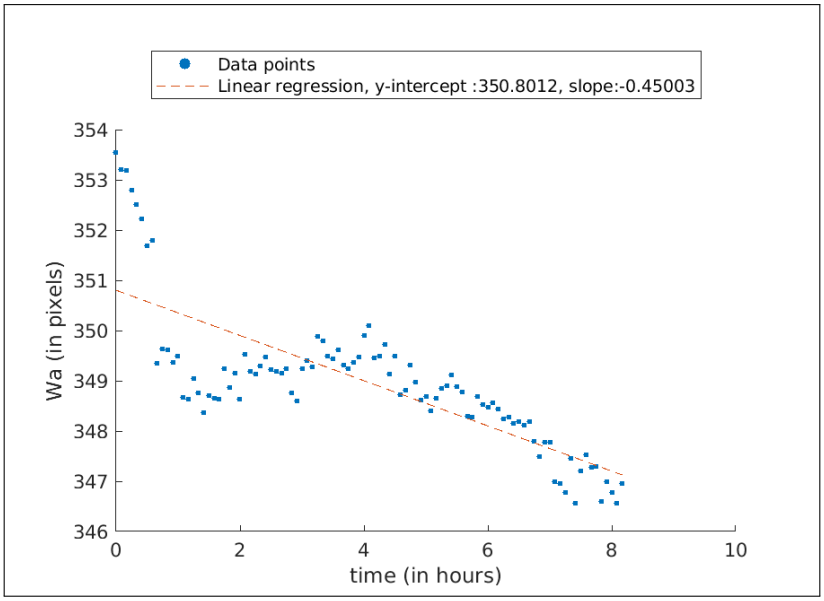

Fig. 3.30: Plot showing the time evolution of the major-axis of the film.

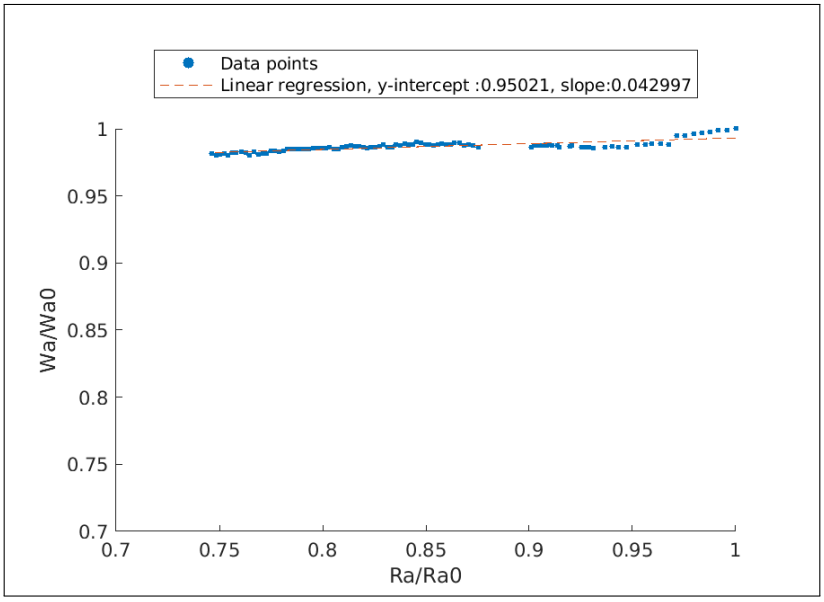

Fig. 3.31: Plot showing evolution of the major-axis of the film with respect to the major-axis of the ball.

Tab. 3.5: Experimental parameter for Fig. 3.31

Expt_Name	Film_ diameter (W_{a0})(in inches)	Film_ thickness (in nm)	Initial_ Ratio (W_{a0}/R_{a0})	Overall Slope	Hours of expt (in hours)
20191125	0.328	426	0.57	0.04	8.17

3.4 Dependence of slope of W_a/W_{a0} versus R_a/R_{a0} plot on W_{a0}/R_{a0} and thickness of the film

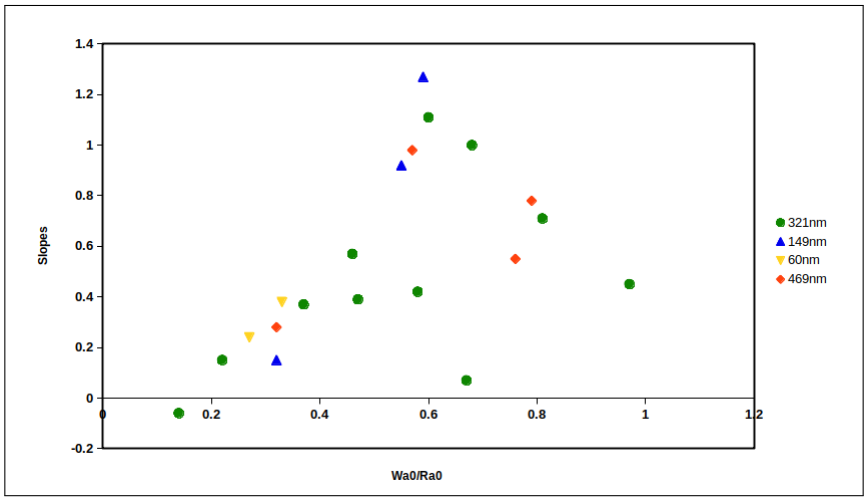

Fig. 3.32: The slope of W_a/W_{a0} versus R_a/R_{a0} curves measured over the range where R_a/R_{a0} changes from 1 to 0.98 plotted here as a function of W_{ao}/R_{a0}. The region beyond 0.6 on the x-axis of this graph contains large noise which we don't understand until now.

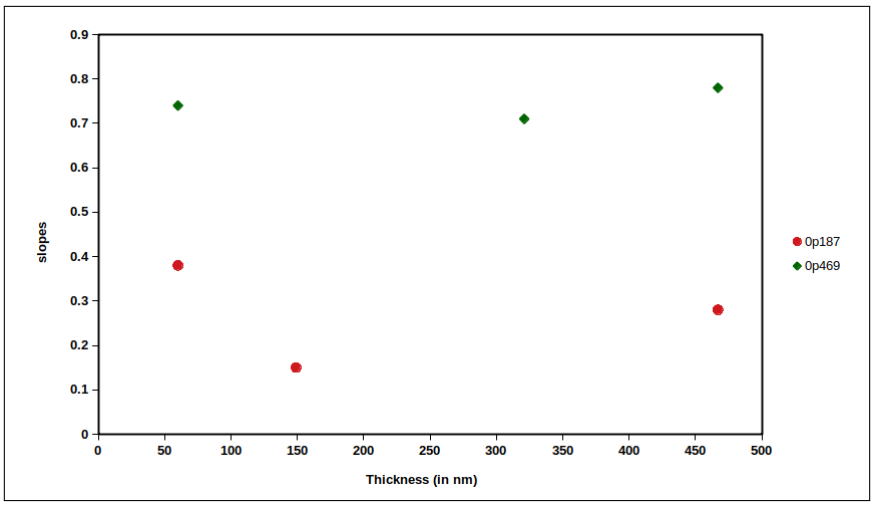

Fig. 3.33: The slope of W_a/W_{a0} versus R_a/R_{a0} curves measured over the range where R_a/R_{a0} changes from 1 to 0.98 plotted here as a function of thicknesses of the film of diameter 0.187 inch and o.469 inch.

Tab. 3.6: The slopes of W_a/W_{a0} Vs R_a/R_{a0} curves measured over the range where R_a/R_{a0} changes from 1 to 0.98 as a function of W_{ao}/R_{a0}.

321nm			**469nm**		
Film size (in inches)	**Wa0/Ra0**	**Slope (0.98 to 1)**	**Film size (in inches)**	**Wa0/Ra0**	**Slope (0.98 to 1)**
0.062	0.14	-0.06	0.187	0.32	0.28
0.125	0.22	0.15	0.328	0.57	0.98
0.203	0.37	0.37	0.437	0.76	0.55
0.25	0.46	0.57	0.469	0.79	0.78
0.25	0.47	0.39	**149nm**		
0.328	0.6	1.11	**Film size (in inches)**	**Wa0/Ra0**	**Slope (0.98 to 1)**
0.328	0.58	0.42	0.187	0.32	0.15
0.375	0.67	0.07	0.312	0.59	1.27
0.375	0.68	1	0.312	0.55	0.92
0.469	0.81	0.71	**60nm**		
0.562	0.97	0.45	**Film size (in inches)**	**Wa0/Ra0**	**Slope (0.98 to 1)**
			0.156	0.27	0.24
			0.187	0.33	0.38

Tab. 3.7: The slopes of W_a/W_{a0} Vs R_a/R_{a0} curves measured over the range where R_a/R_{a0} changes from 1 to 0.98 as a function of thicknesses of the film.

Film diameter = 0.187 inches		**Film diameter = 0.469 inches**	
Thickness (in nm)	**slope**	**Thickness (in nm)**	**slope**
60	0.38	60	0.74
149	0.15	321	0.71
467	0.28	467	0.78

A complete list of all the experiments that have been done can be found in Appendix II

Chapter 4

Additional observations

Here we will look into a few important unusual observations made during this project. The following sections will describe each of those observations independently which will help in studying geometrical effect in-depth as well as it will help in future studies of pattern emergence, dynamics and distribution.

4.1 Anisotropic stick-slip motion of film

While analysis, we found that in large time scale, the overall film compression looks isotropic, but fitting the film with ellipse instead of a circle from the top-view shows that when major axis of the film is stuck to the ball, minor axis slips and vice versa as shown in Fig.4.1. At the current scope of analysis errors, we are sceptical about not having any kind of least count limitation or image analysis errors. In later experiments, we have not analyzed for both major and minor axis of the film. But such analysis will tell about the kind of motion of the film which leads to the specific evolution of the pattern.

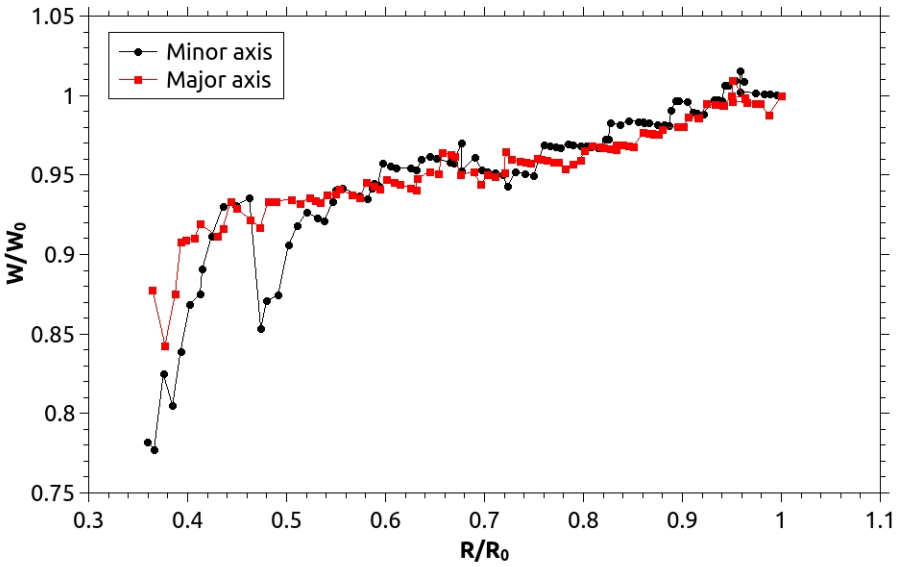

Fig. 4.1: Stick-slip motion of film (not dyed) of thickness = 1403nm and diameter = 0.219 inches. When the major axis plot is flat means film along its major axis is slipping, right at the centre of that region, minor axis becomes vertical i.e. it gets stuck and vice versa.

4.2 Stick-slip event of confined film

In one of our experiments, we found that the film slips suddenly in the experiment and goes back to the initial state with few folds. This happened multiple times in the same experiment as shown in Fig.4.2. However, we did not see many instances of this phenomena in the later experiments, but this might help in understanding the movement of the film. This could also be some kind of disturbance in the experiment in which we are not sure about. Initially, this was the first experiment which suggested to us that the film slips while compression, so we started analysing the rate of compression of film.

Fig. 4.2: Sudden slipping of the film without any dye of thickness = 144nm and diameter = 0.281 inches. The film develops some pattern but later it goes to its initial state by releasing the folds and the same process repeats several times.

4.3 Varieties of W_a/W_{a0} versus R_a/R_{a0} plots

In this whole set of experiments on convex positive Gaussian curvature, we found three different types of W_a/W_{a0} Vs R_a/R_{a0} plots. Few were straight-line curve like one shown in Fig. 4.3, few others were smoothly changing curves like one shown in Fig. 4.4 and rest were having a sharp change in slope values like one shown in Fig. 4.5. We still don't understand the reason behind such a sharp change in slope. But a detailed analysis of the dependence of elastic stress on Gaussian curvature including out-of-plane deformations might reveal the reason behind this too.

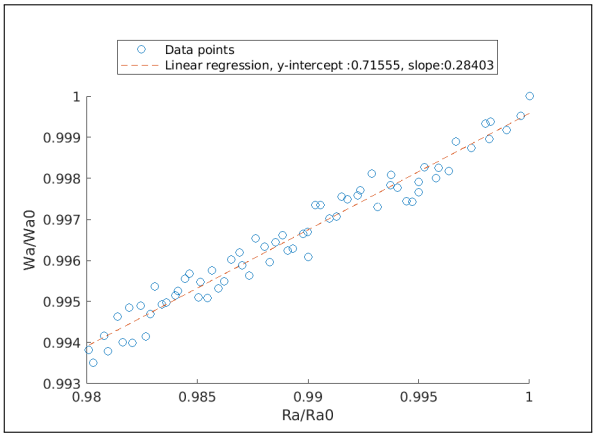

Fig. 4.3: No change in the slope of this curve, film thickness = 467nm

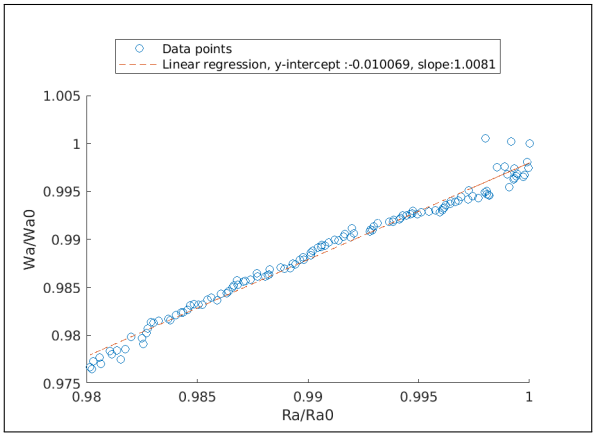

Fig. 4.4: Smooth transition of the slope of this curve, film thickness = 321nm

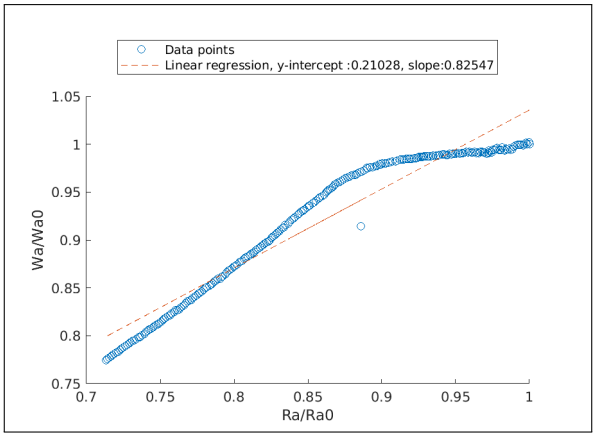

Fig. 4.5: The slope of this curve changes sharply, film thickness = 60nm

4.4 Emergence of various kinds of patterns

In experiments, we found that the pattern can evolve mainly in two different ways as shown in Fig.4.6 and both the ways start from similar initial states and they lead to similar final states. The two different ways in which they evolve are:

1. **Type 1 :** There are radial folds initially, then circumferential folds emerge from the outer side of the film towards the centre of the film.

2. **Type 2 :** There are radial folds initially which reaches the centre of the film by growing and then circumferential folds start emerging from the centre of the film towards the outer side of the film.

Among both the ways, the second one is more commonly found.

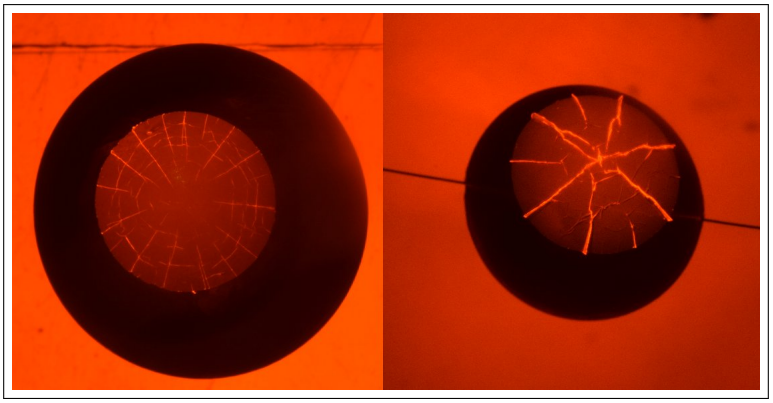

Fig. 4.6: The left image shows the Type 1 pattern evolution and the right image shows the Type 2 pattern evolution

Chapter 5

Analysis and discussion

In this chapter, we will first discuss the fundamentals of elastic energies due to the general deformation of a 2D sheet[10]. In later sections, we will describe the approach we took to explain the dependence of friction on Gaussian curvature of the substrate mathematically with certain assumptions to simplify the calculations.

5.1 Energy and stress required for general deformation

Stretching and bending are the two fundamental modes of 2D sheet deformation.

Energy density in a 2D sheet due to stretching is given by

$$Energy \ = \ \frac{Y}{2}\epsilon^2 \tag{5.1}$$

Where, Y = Stretching modulus, ϵ = Strain

and for bending, it is given by

$$Energy \ = \ \frac{B}{2}\kappa^2 \tag{5.2}$$

Where, B = Bending modulus, κ = Curvature along i^{th} direction.

So, considering a sheet in undeformed state with position vectors of the coordinates of points on sheet,

$$R^o(x,y) = \begin{pmatrix} x \\ y \\ 0 \end{pmatrix} \tag{5.3}$$

In any coordinate system, the metric of the system gives length of a differential element. So, metric for this sheet will be given by $g^o_{ij} = \partial_i R^o . \partial_j R^o$,

Example 5.1. $g_{11} = \partial_x R^o . \partial_x R^o$

$$= \begin{pmatrix} 1 & 0 & 0 \end{pmatrix} \begin{pmatrix} 1 \\ 0 \\ 0 \end{pmatrix}$$

Similarly, the metric will be given by,

$$g^o = \begin{pmatrix} 1 & 0 \\ 0 & 1 \end{pmatrix} \tag{5.4}$$

After deformation, let the position vectors be given as,

$$R(x, y) = \begin{pmatrix} x + u(x, y) \\ y + v(x, y) \\ w(x, y) \end{pmatrix} \tag{5.5}$$

and the corresponding metric will be given by,

$$g = \begin{pmatrix} (1 + u_x)^2 + v_x^2 + w_x^2 & (1 + u_x)u_y + (1 + v_y)v_x + w_x w_y \\ (1 + u_x)u_y + (1 + v_y)v_x + w_x w_y & u_x^2 + (1 + v_x)^2 + w_x^2 \end{pmatrix} \tag{5.6}$$

Where, $\partial_x u = u_x$ convention is used.

So the strain is given by $\epsilon = \frac{g - g^0}{2}$. How strain is equal to the difference in metric tensor is explained in section 2 of Chapter 2 in the following book [22].

Hence, stress required for the above strain can now be obtained from the general Hook's law[23], given as:

$$\sigma_{ij} = \frac{E}{1 + \nu}(\epsilon_{ij} + \frac{\nu}{1 - 2\nu}\epsilon_{kk}\delta_{ij}) \tag{5.7}$$

Where, E = Young's modulus and ν is Poisson ratio.

5.2 Effects of Gaussian curvature on frictional interaction

Consider a thin 2D circular sheet of radius L and of thickness t (t<<L). When it is loaded onto the ball of radius R, the sheet will experience an adhesive and gravitational force

when there is no other external force. Let's assume that gravitational force on the sheet is negligible in comparison to the adhesive force. Assuming that the sheet cannot deform out of the plane when conformed to the substrate, due to this adhesive force the sheet will experience radial stretching and circumferential compression to be able to acquire the shape of the substrate.

Consider a ring of radius x on flat sheet before confinement as shown in Fig.5.1.

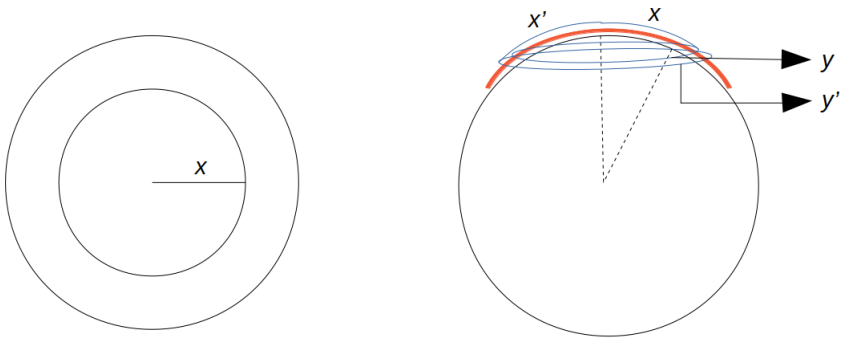

Fig. 5.1: Schematic diagram showing the deformation of a planar sheet when conformed to a spherical substrate.

Say the sheet after confinement gets isotropically stretched by δx.
So, radial strain[24] is given by

$$\alpha = \frac{\delta x}{x} \tag{5.8}$$

New radius of the ring becomes

$$x^{'} = x(1+\alpha) \tag{5.9}$$

Before confinement, the circumference of the circle of radius x was

$$y = 2\pi x \tag{5.10}$$

The angle subtended by the new stretched radius of sheet at the center of the ball is then given by:

$$\theta = \frac{x^{'}}{R} \tag{5.11}$$

So the circumference of the new stretched ring is given by

$$y' = 2\pi R sin(\frac{x^{'}}{R}) \tag{5.12}$$

So, circumferential strain is given by

$$\beta = \frac{y' - y}{y} = R\frac{sin(\frac{x'}{R})}{x} - 1 \tag{5.13}$$

$$\beta = R\frac{sin(\frac{x(1+\alpha)}{R})}{x} - 1 \tag{5.14}$$

Now since we have both radial and circumferential strain, the total elastic energy required for producing the strain is given by

$$U_e = U_r + U_c \tag{5.15}$$

$$U_e = [\frac{1}{2}Y\alpha^2 + \frac{1}{2}Y\beta^2]\pi L^2 \tag{5.16}$$

Initial area of the sheet is given by

$$A = \pi L^2 \tag{5.17}$$

After confinement, area of sheet becomes

$$\int_0^{A'} dA' = \int_0^{L(1+\alpha)} 2\pi x(1+\alpha)dx \tag{5.18}$$

$$\implies A' = \pi L^2(1+\alpha)^2 \tag{5.19}$$

Now, as the sheets get stretched, area of the sheets increases by a small amount, and as the total adhesion energy depends on the area of the sheet, increase in adhesion energy due to confining the sheet onto the ball is given by

$$U_a = -\gamma(A' - A) \tag{5.20}$$

$$U_a = -\gamma(\pi L^2(1+\alpha) - \pi L^2) \tag{5.21}$$

$$U_a = -2\gamma\pi L^2\alpha \tag{5.22}$$

Now, the total energy of the system is given by the sum of equation 5.16 and 5.22

$$U = U_e + U_a \tag{5.23}$$

$$U = [-2\gamma\alpha + \frac{1}{2}Y\alpha^2 + \frac{1}{2}Y\beta^2]\pi L^2 \tag{5.24}$$

At equilibrium, the total energy of the system can be found by minimizing the equation 5.24.

$$\frac{\partial U}{\partial \alpha} = [-2\gamma + Y\alpha + Y\beta\frac{\partial \beta}{\partial \alpha}]\pi L^2 \tag{5.25}$$

At equilibrium, $\frac{\partial U}{\partial \alpha} = 0$ So,

$$-2\gamma + Y\alpha + Y(R\frac{sin(\frac{x(1+\alpha)}{R})}{x} - 1)\frac{\partial(R\frac{sin(\frac{x(1+\alpha)}{R})}{x} - 1)}{\partial \alpha} = 0 \tag{5.26}$$

$$\implies -2\gamma + Y\alpha + Y(R\frac{sin(\frac{x(1+\alpha)}{R})}{x} - 1)cos(\frac{x(1+\alpha)}{R}) = 0 \tag{5.27}$$

$$\begin{aligned}\implies -2\gamma + Y\alpha + Y(R\frac{sin(\frac{x}{R})cos(\frac{x\alpha}{R}) + cos(\frac{x}{R})sin(\frac{x\alpha}{R})}{x} - 1)\\ (cos(\frac{x}{R})cos(\frac{x\alpha}{R}) - sin(\frac{x}{R})sin(\frac{x\alpha}{R})) = 0\end{aligned} \tag{5.28}$$

Now, since $\alpha < 1$ and $\frac{x}{R} < 1$, $\alpha\frac{x}{R} << 1$, so we can expand sine and cosine as follows

$$cos(\frac{\alpha x}{R}) = 1 + \frac{1}{2!}(\frac{\alpha x}{R})^2 \tag{5.29}$$

$$sin(\frac{\alpha x}{R}) = \frac{\alpha x}{R} - \frac{1}{3!}(\frac{\alpha x}{R})^3 \tag{5.30}$$

So, equation 5.28 is now given by

$$\begin{aligned}-2\gamma + Y\alpha + Y(R\frac{(\frac{x}{R} - \frac{1}{3!}(\frac{x}{R})^3)(1 + \frac{1}{2!}(\frac{\alpha x}{R})^2) + (1 + \frac{1}{2!}(\frac{x}{R})^2)(\frac{\alpha x}{R} - \frac{1}{3!}(\frac{\alpha x}{R})^3)}{x} - 1)\\ ((1 + \frac{1}{2!}(\frac{x}{R})^2)(1 + \frac{1}{2!}(\frac{\alpha x}{R})^2) - (\frac{x}{R} - \frac{1}{3!}(\frac{x}{R})^3)(\frac{\alpha x}{R} - \frac{1}{3!}(\frac{\alpha x}{R})^3)) = 0\end{aligned} \tag{5.31}$$

On simplification, we get,

$$\sim -2\gamma + Y\alpha + Y(\alpha - \frac{1}{6}(\frac{x}{R})^2) = 0 \tag{5.32}$$

$$\implies \alpha = \frac{2\gamma + Y(\frac{1}{6}(\frac{x}{R})^2)}{2Y} \tag{5.33}$$

Thus, when the stretching obeys the functional form in equation 5.33, the energy of the sheet is minimized and is provided by the adhesive force from the substrate so that the film can confine to the substrate.

If out of the plane deformations are considered, the total equilibrium energy will reduce further. But to do that one needs to understand the patterns well and for that one should be able to classify the patterns. At this stage of this project, we are ignoring the bending energy due to out-of-plane deformations.

This strain α depends on Gaussian curvature of the underlying substrate ball. So,

The stress builds on the sheet due to this strain will also depend on underlying Gaussian curvature of the substrate.

If there is a tangential force on the surface for instance surface tension in case of a liquid drop, it will contribute to a normal force towards the centre of the drop. This is called Laplace pressure. By solving the case of a liquid drop, it can be seen that the Laplace pressure depends on the sum of principal Curvatures of the drop. Similarly, we can now calculate the Laplace pressure due to this elastic stress which will be directed normally inwards of the ball which will lead to an increase in the frictional interaction.

Now since the increase in Gaussian curvature would cause an increase in stress in the sheet. This would cause the frictional interaction between the sheet and the substrate beneath it to increase with time since Gaussian curvature of the ball is a function of time in this case.

Numerical analysis for the energy minimization's and strains is provided in Appendix I.

Chapter 6

Conclusions and future directions

6.1 Conclusions

From the data in subsection 3.3.1 we saw that the rate of slipping of the film increases as the radius of the underlying sphere becomes smaller. This result is reproducible in multiple experiments and it suggests that the frictional interaction between the film and the ball is dependent on the curvature of the underlying substrate. We saw in experiment on a flat substrate that the film slipped throughout the experiment until it touches the boundary of the substrate where it encounters the spherical surface of the ball. Now, to clarify whether it was the mean curvature or the Gaussian curvature which was important, we did experiments on cylindrical substrates. There also we found that the film slips on the substrate similarly as seen on the flat substrate. This series of experiments confirm that the effective frictional interaction between a thin film and a substrate depends on the Gaussian curvature of the substrate. So, the next question is how can the frictional interaction be coupled to the Gaussian curvature of the substrate? For this we did one more experiment which sheds light on this connection: when the thin film is placed on a concave substrate, we don't see any pattern evolution although there are initial folds similar to that of the convex case since the film slips like on the substrate of zero Gaussian curvature. So, we arrive at the following picture: in both convex as well as concave case the film gets stretched and that stretching force has a component along the normal direction which can either lead to increase or decrease in the effective adhesion and hence friction based on its direction whether it is directed into the surface (in convex positive case) or out of the surface (in concave positive case).

The argument presented above is backed by our calculations presented in section 5.2 which are are numerically solved and presented in Appendix I. From the numerical

analysis, it can be inferred that there exists a minimum elastic energy which depends on $l = W_{a0}/R_{a0}$. And calculations done above in section 5.2 show that it depends on l^2. The strain plots of α and β show that up to $l = 1$, the regime where we are working, there is radial stretching which increases with l and there is circumferential compression which also increases with l. This analysis is valid for a given instant. Since Gaussian curvature in our experiment is time dependent, the time-varying numerical analysis will show that equilibrium energy shifts towards the right with increasing l. This implies that elastic stress on film will increase with time due to increasing difference between the Gaussian curvature of the sheet and the ball.

From experiments, we also noticed that as the Gaussian curvature of the substrate is increased in convex direction, the friction between the film and the ball increases. In small time, the pattern doesn't evolve much, and the film slips almost at the same rate for various thicknesses of the film as it can be inferred from Fig. 3.33. And from Fig. 3.32 it can be inferred that the film sticks more to the substrate when the film size is increased. Both these plots suggest that accumulating elastic energy due to an increase in deformation increases the effective adhesion which in turn leads to increase in frictional interaction.

6.2 Future directions

In day to day life, we often see crumpling of a sheet which is confined to a surface with Gaussian curvatures, like skin-tissue on the human body, outer covering on objects like lamination, earth crust and the skin of fruits. It is therefore important to understand how various wrinkling patterns form on these confined sheets [8]. This is an area of intense research activities and many questions remain open and actively pursued. In common crumpling experiments, researchers first crumple the sheet and then reopen it to analyse the patterns or they try to analyse the ridge and valley patterns by a scanning method [25] [4]. This approach has helped us understand certain statistical aspects of the final crumpled state. In contrast, our experiment allows observing the dynamics as the individual folds and ridges form with increasing compression, as well as to measure quantities for them without disturbing or reopening the ongoing process. Rather a reopening process can be explored as a completely different aspect here in this experiment. A thin film will usually stick on to itself and deforms plastically if it comes in contact with itself(in 100nm thickness scale), but we found that even after completely getting crumpled it reopens into a flat sheet with some crease patterns on it when the crumpled piece is placed on top of the water. What kind of pattern evolution

makes it possible to arrange in a particular way that even a plastically deformed and crumpled material can also reopen? It will be further useful to confirm the isotropy of film compression and understand the motion of the film. This will provide us with information about how this particular type of pattern develops on surfaces. In this way, a detailed study of the patterns formed could demystify the secrets of crumpling.

While trying to understand the crumpling process, as described in section 3.2 we found that due to simultaneous imaging of film and ball which lie on two different planes, there exist two different values of magnification for the two. This introduces some error in our measurement of the slope of the curve in the plot W_a/W_{a0} versus R_a/R_{a0}. So, to resolve this problem either one can calculate and compensate for it or make some experimental changes. We did some experimental changes by hanging the ball through a wire. This fixes the ball's distance from the top camera, so part of the problem gets resolved but the film distance from the camera still changes and it stays on a plane other than that of the ball's centre plane. Thus it remains a challenge to analyze the top view images without which patterns cannot be studied quantitatively. Recently, our work in this direction suggested that it might be possible to account for this issue by using cross-ratio for the images. One needs to improvise the experimental setup and the make the necessary compensation in analysis to correct for this error arising out of differential magnifications for the film and the ball.

While exploring all Gaussian curvatures to understand the dependence of frictional interaction between the film and the ball on Gaussian curvatures, we couldn't explore the negative and elliptical Gaussian curvatures due to experimental challenges which we couldn't overcome due to lack of hydrogel cutting instruments, information to prepare desired hydrogel surfaces, time and proper setup to analyze from top-view. Experimenting on such Gaussian curvatures will further strengthen our knowledge on this relation between friction and the Gaussian curvatures. This will also be useful to validate our results and remove chances of biases towards observations. It will help analyse the complete system without any assumption because from the outcome of our analysis, we believe that our result is valid for all kinds of Gaussian curvature but our final expressions for strains shows dependence on product of symmetric principal curvatures. Our analysis assumes that there is no out-of-plane buckling of the film. If we will consider the out-of-plane buckling, the minimum equilibrium energy will decrease further. Exploration of this question is a critical confirmation required for the dependence of friction on Gaussian curvature of the substrate.

Appendices

I Verification of energy minimization

This analysis was done in Mathematica.

Ua[α_]:=α^2; (* Radial stretching energy*)

β[α_, l_]:=$\frac{\text{Sin}[l(1+\alpha)]}{l}$ − 1; (* circumferential strain*)

Ub[α_, l_]:=$\beta[\alpha, l]^2$; (* circumferential compression energy*)

U[α_, l_]:=Ua[α] + Ub[α, l]; (* Total elastic energy*)

Plot[$U[\alpha, 0.3]$, {α, 0, 0.02}, AxesLabel → {α, $U[\alpha, l]$}]

(* Plotting total elastic energy as a function of radial strain α*)

β[0.0075, 0.3]

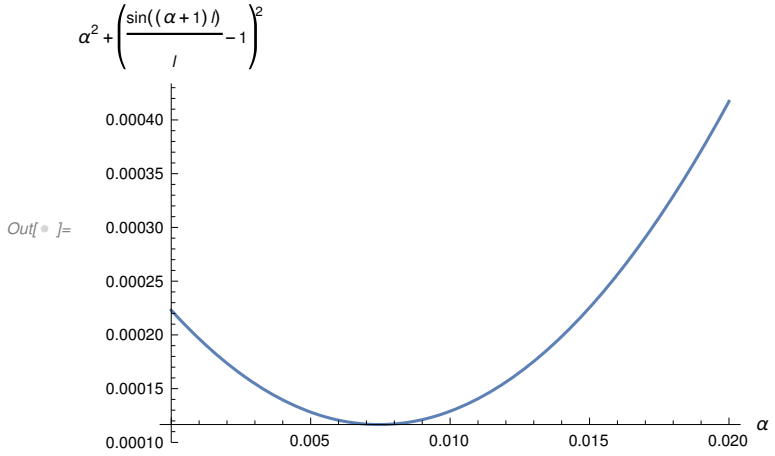

Fig. .1: Total elastic energy as a function of radial strain for $W_{a0}/R_{a0} = 0.3$

$(*\beta[0.0075, 0.3]*) = -0.00777012$

F[α_, l_]:=$D[U[x, a], x]$/.{$x \to \alpha, a \to l$};

(* Differentiating total elastic energy to get equilibrium strain*)

α[l_]:=α/.FindRoot[$F[\alpha, l] == 0$, {α, 0.0}];

(* Finding solution for α as a function of l.*)

α[0.65]

Plot[{$\alpha[l], \beta[\alpha[l], l]$}, {$l$, 0, 1}, AxesLabel → {$l$, Strain}, PlotLabels → {α, β}]

$(*\alpha[0.65]*) = 0.0333552$

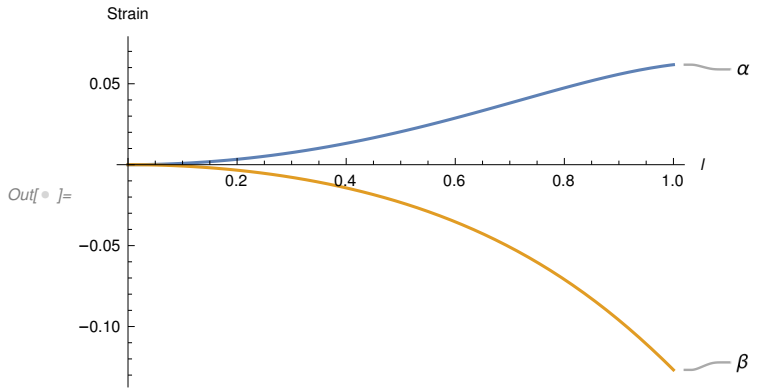

Fig. .2: Radial and circumferential strain as a function of $W_{a0}/R_{a0} = 0.3$

II List of experiments

Tab. .1: 4wt% films, Positive convex Gaussian curvature

Expt_Name	Types_of_ Analysis_done	Film_ diameter (W_{ao}) (in inches)	Film_ thickness (in nm)	Initial_ Ratio (W_{a0}/R_{a0})	Initial Slopes	Later Slopes	Overall Slopes	Hours of expt. (in hours)	Slope 0.98 to 1	time to reach 0.98 (in hours)
20200101	ellipsefit	0.062	321	0.14	0.28	1.47	1	4	0.04	0.685
20191221	ellipsefit	0.125	321	0.22	0.06	0.06	0.06	2.4	0.13	1.48
20191220	ellipsefit	0.203	321	0.36	0.1	0.42	0.5	2.2	0.41	1.12
20191222	ellipsefit	0.25	321	0.45	0.5	0.88	0.7	2.55	0.55	1.6
20191228	ellipsefit	0.25	321	0.46	0.44	0.68	0.9	4.3	0.337	0.64
20200102	ellipsefit diff_1/R^2_same_a/R	0.281	321	0.53	0.15	0.44	0.31	0.98	0.315	0.5
20200102	ellipsefit diff_1/R^2_same_a/R	0.297	321	0.53	0.39	0.37	0.5	0.97	0.5	0.5
20191221	ellipsefit thickness_vs_slope	0.328	321	0.55	0.37	0.68	0.52	2.54	0.41	1.6
20200107	Circularfit Ellipsefit diff_1/R^2_same_a	0.328	321	0.556	0.82	0.82	0.82	3.32	0.82	_
20191219	ellipsefit thickness_vs_slope	0.328	321	0.56	1	1	1	2.5	1.05	2.27
20200102	ellipsefit diff_1/R^2_same_a/R	0.328	321	0.58	0.33	0.33	0.33	0.98	0.187	0.75
20200107	Circularfit Ellipsefit diff_1/R^2_same_a	0.328	321	0.62	0.47	0.47	0.47	3.09	0.467	3.07
20200107	Circularfit Ellipsefit diff_1/R^2_same_a	0.328	321	0.67	0.17	0.72	0.59	5.9	0.168	1.66
20191222	ellipsefit	0.375	321	0.62	-0.08	1.4	1.26	3	1.22	2.46
20191224	ellipsefit	0.375	321	0.63	0.93	0.93	0.93	2.9	0.82	2.06
20191219	ellipsefit	0.469	321	0.73	0.64	0.64	0.64	3.1	0.61	1.945
20191223	Circularfit	0.562	321	0.83	0.4	0.4	0.4	3.55	0.345	1.55

Tab. .2: Positive convex Gaussian curvature

Expt_Name	Types_of _Analysis	Film_ thickness (in wt%)	Film_ diameter (W_{ao})(in inches)	Film_ thickness (in nm)	Initial_ Ratio (W_{a0}/R_{a0})	Initial Slopes	Later Slopes	Overall Slopes	Hours of expt (in hours)	Slope 0.98 to 1
20191218	Ellipsefit	1	0.156	60	0.27	-0.01	0.92	0.74	3.05	
20200204	Ellipsefit	1	0.187	60	0.33	0.19	1.1	0.78	20.4	
20191219	Circularfit manual analysis	1	0.469	60	0.81	0.27	3.13	1.27	2.5	
20200205	Ellipsefit	2	0.187	149	0.32	0.19	0.89	0.84	34	0.116
20200118	Ellipsefit	2	0.203	149	0.33	1.03	1.03	1.03	13.35	0.67
20200118	Ellipsefit	2	0.203	149	0.19	0.19	0.19	0.19	13.35	0.81
20191223	ellipsefit thickness_vs_slope	2	0.312	149	0.55	1.2	1.2	1.2	3	1.17
20200115	ellipsefit top_view side_view thickness_vs_slope	2	0.312	149	0.52	0.8	0.8	0.8	2	0.78
20191226	Ellipsefit	5	0.187	467	0.32	0.26	0.71	0.43	2.95	
20191221	ellipsefit thickness_vs_slope	5	0.328	467	0.54	0.91	0.91	0.91	4.54	
20191226	Ellipsefit	5	0.437	467	0.7	0.64	0.64	0.64	3.35	
20191220	Ellipsefit	5	0.469	467	0.71	0.69	0.69	0.69	3.46	
20191011	-	5	0.562	426	0.7	0.03	1	0.85	42	
20191021	-	5	0.812	426	0.94	0.61	1.09	0.72	80	

Tab. .3: Flat zero Gaussian curvature

Expt_Name	Types_of_ Analysis_done	Film_ thickness (in wt%)	Film_ diameter (W_{ao})(in inches)	Film_ thickness (in nm)	Initial_ Ratio (W_{a0}/R_{a0})	Initial Slopes	Later Slopes	Overall Slopes	Hours of expt (in hours)
20191107	Circularfit manual analysis	1	0.328	60	0.57	0.04	0.04	0.04	13
20200121	Ellipsefit	1	0.187	60	0.33	0.08	0.08	0.08	19.2
20200213	Ellipsefit	1	0.187	60	0.35	0	0.67	0.64	8.3
20191102	Circularfit manual analysis	5	0.281	426	0.47	0.06	0.06	0.06	20.75
20191105	Circularfit manual analysis	5	0.328	426	0.58	0.26	0.26	0.26	12.67
20191104	Ellipsefit	5	0.328	426	0.58	0.03	0.03	0.03	12.3
20200211/00am	Ellipsefit	2	0.328	149	0.5	0.76	0.76	0.76	10.3
20200211/11am	Ellipsefit	2	0.328	149	0.6	0.81	0.81	0.81	16.2

Tab. .4: Positive concave Gaussian curvature

Expt_Name	Types_of_ Analysis	Film_ thickness (in wt%)	Film_ diameter (W_{ao})(in inches)	Film_ thickness (in nm)	Initial_ Ratio (W_{a0}/R_{a0})	Slopes	Hours of expt (in hours)
20191125	Ellipsefit	5	0.328	426	0.57	0.04	8.17

Tab. .5: Cylindrical zero Gaussian curvature

Expt_Name	Types_of_ Analysis	Film_ thickness (in wt%)	Film_ diameter (W_{a0})(in inches)	Film_ thickness (in nm)	Initial_ Ratio (W_{a0}/R_{a0})	Initial Slopes	Later Slopes	Overall Slopes	Hours of expt (in hours)	Slopes 098 to 1	Ball colour
20200120	Ellipsefit	1	0.187	60	0.318	0.1	0.97	0.54	32	0.04	purple
20200119	Ellipsefit	1	0.187	60	0.32	0.19	1.82	0.3	19.3	0.17	purple
20200126	Ellipsefit	1	0.187	60	0.33	0.14	0.14	0.14	21.7	0.17	purple
20191204	Ellipsefit	5	0.328	426	0.51	0.07	0.07	0.07	13.76	0.11	

III Camera and laser control through Arduino UNO

```
// Reference: https://www.christidis.info/index.php/personal-projects/
//arduino-nikon-infrared-command-code

#define LEDpin 13



void takePhoto(void) {
int i;
for (i = 0; i < 76; i++) {
digitalWrite(LEDpin, HIGH);
delayMicroseconds(7);
digitalWrite(LEDpin, LOW);
delayMicroseconds(7);
}
delay(27);
delayMicroseconds(810);
for (i = 0; i < 16; i++) {
digitalWrite(LEDpin, HIGH);
delayMicroseconds(7);
digitalWrite(LEDpin, LOW);
delayMicroseconds(7);
}
delayMicroseconds(1540);
for (i = 0; i < 16; i++) {
digitalWrite(LEDpin, HIGH);
delayMicroseconds(7);
digitalWrite(LEDpin, LOW);
delayMicroseconds(7);
}
delayMicroseconds(3545);
for (i = 0; i < 16; i++) {
digitalWrite(LEDpin, HIGH);
delayMicroseconds(7);
digitalWrite(LEDpin, LOW);
delayMicroseconds(7);
}
Serial.println("taken" );
}

```

```
41              void setup() {
42
43              pinMode(LEDpin, OUTPUT); //camera
44              Serial.begin(9600);
45              pinMode(8,OUTPUT); //laser
46              pinMode(12,OUTPUT); //laser
47
48              }
49
50              void loop() {
51              // put your main code here, to run repeatedly:
52              digitalWrite(8,HIGH);
53              digitalWrite(12,HIGH);
54              Serial.print("Laser is on.");
55              delay(1000);
56              takePhoto();
57              delay(24000);
58              digitalWrite(8,LOW);
59              digitalWrite(12,LOW);
60              Serial.print("Laser is off.");
61              delay(35000);
62              }
```

IV Camera and laser control through Laptop using Python and Arduino

Python part -

```
1               # Libraries
2               import serial as sl
3               import time
4               import datetime
5               import glob
6               import cv2
7
8               s = sl.Serial('/dev/ttyACM0',9600)
9               # s is the port where Arduino is waiting to receive command from this code
10
11              countcheck = 0
12              # This is a flag which informs the code whenever a new image arrives
13
14
```

```
15                  k = datetime.datetime.now()
16                  # This variable keeps time when the image arrived in the folder.
17
18                  times = []
19                  # This array keeps the record of times when Laser got a signal.
20
21                  try:
22                  while True:
23                  n = len(glob.glob1("/home/zorawar/Desktop/camlive/","*.JPG"))
24                  # 'n' keeps a count of total number of images in the folder at this instant
25
26                  if n - countcheck == 1:
27                  # when image arrives
28
29                  s.write('0'.encode())
30                  # Command '0' string is sent to the Arduino.
31
32                  t = datetime.datetime.now()
33
34                  k = t
35                  # Updates the time
36
37                  times.append(str(t))
38                  # Updated time is saved in the array
39
40                  countcheck = n
41                  # Flag value is raised to variable 'n' to detect next image
42
43                  t1 = datetime.datetime.now()
44                  # New time instant is generated
45
46                  m = t1-k
47                  print(m.total_seconds())
48                  # time difference between old and new time is found and printed
49
50                  print(countcheck)
51                  # Count of current number of images in folder is printed
52
53                  if m.total_seconds()>700:
54                  break
55                  # This condition detects completion of experiment or sync error.
56                  except KeyboardInterrupt:
57                  pass
58
59                  file = open("/home/zorawar/Desktop/camlive/times.txt","w+")
60                  # A file is created in the folder
61
62                  for i in times:
```

```
63                  file.write(i+"\n")
64                  file.close()
65                  # It writes all the time instances in this .txt file and saves it.
```

Arduino part- It receives the command from the running python code and controls the laser.

```
1                   char m;
2                   // It creates a variable of character type
3
4                   void setup() {
5                   // put your setup code here, to run once:
6                   Serial.begin(9600);
7                   // It switches on the serial port
8                   pinMode(8,OUTPUT);
9                   // This pin of Arduino will be used to communicate with the laser
10
11                  while (!Serial) {
12                  ; // wait for serial port to connect. Needed for native USB
13                  }
14                  }
15
16                  void loop() {
17                  // put your main code here, to run repeatedly:
18                  if(Serial.available()>0)
19                  // It says if serial port is found open
20                  {
21                  m = Serial.read();
22                  // The command coming from serial is saved in this variable(which if
23                  you remember is '0')
24                  }
25                  if(m == '0')
26                  {
27                  digitalWrite(8,LOW);
28                  digitalWrite(12,LOW);
29                  Serial.print("Laser is off.");
30                  m = '1';
31                  delay(595000);
32                  // if it receives command from port, it switches both laser off, and
33                  //resets the variable and waits for given interval of time(1sec = 1000)
34                  }
35
36                  digitalWrite(8,HIGH);
37                  digitalWrite(12,HIGH);
38                  Serial.print("Laser is on.");
39                  delay(5000);
40                  // After that it switches on both the laser.
41                  }
```

V Image analysis MATLAB codes

V.1 Imaging time extraction (time.m)

```
clc;
clear;
close all;
count=1;

imagelist = dir(fullfile('*.JPG'));
path = pwd;
fol = [path '/dynamics/'];
for i=1:(length({imagelist.name}) - 1)
a = imfinfo(imagelist(i).name);
dt1 = datestr(datenum(a.DateTime,'yyyy:mm:dd HH:MM:SS'));
dt1 = datevec(dt1);
if count == 1
k = dt1;
end
a = imfinfo(imagelist(i+1).name);
dt2 = datestr(datenum(a.DateTime,'yyyy:mm:dd HH:MM:SS'));
dt2 = datevec(dt2);
out=[str2double(imagelist(i).name(5:9))
etime(dt2,dt1)];
dlmwrite([fol 'time.ods'],out,'-append');
% (image number, time elapsed from its previous image)
count = 2;
end
count = 1;
for i=1:length({imagelist.name})
a = imfinfo(imagelist(i).name);
dt1 = datestr(datenum(a.DateTime,'yyyy:mm:dd HH:MM:SS'));
dt1 = datevec(dt1);
if count == 1
k = dt1;
end
out1=[str2double(imagelist(i).name(5:9))
dt1 etime(dt1,k)];
dlmwrite([fol 'timestamps.ods'],out1,'-append');
```

```
36                  % (image number, YYYY, MM, DD, HH, MM, SS, time elapsed from first image)
37                  count = 2;
38                  end
```

V.2 For top view

V.2.0 regionellipse.m

```
clc;
clear;
close all;

path = pwd;                                                    % path of current file
fol = [path '/cropped/'];                                      % path of data folders


% Naming Conventions_____________________________________________________
colorim = ['1DSC_'; '2DSC_'];                                  % 1 balls, 2 films
binim = ['bb'; 'bf'];                                          % 1 balls, 2 films
detectim = ['eb';'ef'];                                        % 1 balls, 2 films
excelname = ['b.ods' ;'f.ods'];                                % crude result saving file

% Creates folder to save data as data%d inside ../cropped/
for k= 1:20
    if 7~=exist([fol 'data' int2str(k)],'dir')
        mkdir ([fol 'data' int2str(k)])
        fol1 = [fol 'data' int2str(k) '/'];
        break
    end
end

colorimlis = [dir(fullfile(fol, [colorim(1,:) '*.tif'])) dir(fullfile(fol, [colorim(2,:) '*.tif']))];    % [ball_im_list  film_im_list]
```

```
25 binimlis = [dir(fullfile(fol, [binim(1,:) '*.tif'])) dir(fullfile(fol, [binim(2,:) '*.tif']))];      % [ball_binim_list  film_binim_list]
26
27 count=1;   % count flag
28 for i=1:length(colorimlis(:,1))
29     for l = 1:2
30         im=imread([fol colorimlis(i,l).name]);
31         imb = imread([fol binimlis(i,l).name]);
32         im3=imsharpen(im(:,:,1));
33
34         % regionprops to detect ball and film
35         detect = regionprops('table',imb,'Centroid','MajorAxisLength','MinorAxisLength','Orientation','Eccentricity','Area');
36         bestFits = [detect.Centroid(:,1) detect.Centroid(:,2) detect.MajorAxisLength detect.MinorAxisLength detect.Orientation
37         detect.Area];
38         [value,index] = max(bestFits(:,6));%finds maximum area detected ellipse
39
40         % Ploting detected region
41         implot = figure;
42         imshow(im)
43         t = linspace(0,2*pi,50);
44         hold on
45         a = bestFits(index,3)/2;
46         b = bestFits(index,4)/2;
47         Xc = bestFits(index,1);
48         Yc = bestFits(index,2);
49         phi = deg2rad(-bestFits(index,5));
50         x = Xc + a*cos(t)*cos(phi) - b*sin(t)*sin(phi);
51         y = Yc + a*cos(t)*sin(phi) + b*sin(t)*cos(phi);
52         plot(x,y,'g','Linewidth',1)
53         hold off
54         imwrite(imb,[fol1 detectim(l,:) binimlis(i,l).name]);
55         saveas(implot,[fol1 detectim(l,:) colorimlis(i,l).name]);
```

```
56
57
58          out=[str2double(colorimlis(i).name(6:9)) bestFits(index,1) bestFits(index,2) bestFits(index,3) bestFits(index,4)
59          bestFits(index,5)];
60          dlmwrite([fol1 excelname(l,:)],out,'-append'); % [ image_no. x0 y0 a b alpha]
61      end
62      count=count+1
63      close all;
64  end
65
66  load handel.mat; % notification music
67  nBits = 16;
68  sound(y,Fs,nBits);
```

V.2.0 analysis.m

```
1   clc;
2   clear;
3   close all;
4   % Selecting the data folder to analyze_____________________________________
5   path = pwd;                                                    % path of current file
6   fol = [path '/cropped/'];                                      % path of data folders
7   files = dir(fol);
8   for i= 1: length( [files.isdir])
9       subFolders1 = files(i).isdir;
10      if subFolders1==1
11          subFolders = files(i).name;
12          disp(subFolders)
13      end
14  end
```

```
prompt = 'Which folder do you want to analyze? (as dataint):';
data = input(prompt,'s');
fol1 = [fol data '/'];                                                    % path of data files

% Reading data files_____________________________________________________________________________________________
t = dlmread('timestamps.ods');                                  % time stamps file [im.no, YYYY,MM,DD,HH,MM,SS,elapsetime]
b = dlmread([fol1 'b.ods']);                                      % ball maj/min/rad file [image_no. x0 y0 a b alpha]
f = dlmread([fol1 'f.ods']);                                      % film maj/min/rad file [image_no. x0 y0 a b alpha]

% Compansating film radius_____________________________________
compmaj = [];
time = t(:,8)./3600;
for i=1:length(b)
    compmaj = [compmaj;b(i,4)* asin(f(i,4)/b(i,4))];
end

% Naming concentions and labels of plots_______________________________
figname = ['t_vs_Ra'; 't_vs_Wa'];
pngname = ['t_vs_Ra.png'; 't_vs_Wa.png'];
labels = ['Ra (in pixels)'; 'Wa (in pixels)'];

% Plotting of time Vs ball and time Vs film_____________________________
intercept = [];
slope = [];
Y1 = [b(:,4) compmaj];
for j= 1:2% line 83 to 99 saves linear regression of time-vs-ball and time-vs-film
    h(j) = figure;
    X = [ones(length(time),1) time];
    Y = Y1(:,j);
    beta = X\Y;
    linearreg = X*beta;
```

```
    scatter(time,Y)
    hold on
    plot(time,linearreg,'--')
    xlabel('time (in hours)');
    ylabel(labels(j,:))
    legend('Data points',['Linear regression,' ' y-intercept :' num2str(beta(1)) ', slope:' num2str(beta(2))],'Location','northoutside')
    intercept = [intercept beta(1)];
    slope = [slope beta(2)];
    savefig(h(j),[fol1 figname(j,:)])
    saveas(h(j),[fol1 pngname(j,:)])
end

% Normalizing ball and film radius___________________________
normb = b(:,4)./b(1,4);                                % b(i,4)/intercept(1)];
normf = compmaj(:)./compmaj(1);                % compmaj(i)/intercept(2)];


% Extracting analyzed data file_____________________________________________________
head={'image_name ', 'Ball_major_axis_Ra','Ball_minor_axis_Rb ',  'Ball_Center_x ', 'Ball_Center_y ', 'film_major_axis_ra ' ,
'film_minor_axis_rb ' ,'Film_Center_x ' ,'Film_Center_y ' ,'compansated_film_Wa ' ,'normalized_ball_RabyRa0 ', 'norm_film_WabyWa0 ',
'Time_in_hours '}; %  headings for analyzed excel file
out=table(b(:,1), b(:,4) ,b(:,5),b(:,2) ,b(:,3) ,f(:,4) ,f(:,5),f(:,2) ,f(:,3) ,compmaj ,normb ,normf ,time,'VariableNames',head);
%  data for analyzed excel file
writetable(out,[fol1 'emajdata.xls']);

% Ploting w/w0 Vs Ra/Ra0_____________________________________________________________
normb1=normb(and(normb>=0.0,normb<=1.1));      % Set lower and upper limit
normb2=normb(normb>1.1);                                    % Set upper limit
h(3) = figure;
X = [ones(length(normb1),1) normb1];
beta = X\normf(length(normf)-length(normb1)-length(normb2)+1:length(normf)-length(normb2));
```

```
linearreg = X*beta;
scatter(normb1,normf(length(normf)-length(normb1)-length(normb2)+1:length(normf)-length(normb2)))
hold on
plot(normb1,linearreg,'--')
xlabel('Ra/Ra0');
ylabel('Wa/Wa0')
legend('Data points',['Linear regression,' ' y-intercept :' num2str(beta(1)) ', slope:' num2str(beta(2))],'Location','northoutside')
savefig(h(3),[fol1 'Ra_by_Ra0_Vs_Wa_by_Wa0'])
saveas(h(3),[fol1 'Ra_by_Ra0_Vs_Wa_by_Wa0.png'])

% Saving analyzed results_____________________________________________________
initratio = compmaj(1)/b(1,4);                                          % initial film to ball ratio
head1 = {'slope_of_t_Vs_Ra','y_intercept_of_t_Vs_Ra' ,'slope_of_t_Vs_Wa','y_intercept_of_t_Vs_Wa', 'slope_of_Ra_by_Ra0_Vs_Wa_by_Wa0',
'y_intercept_of_Ra_by_Ra0_Vs_Wa_by_Wa0','Wa_by_Ra_initial'};
prop = table(slope(1),intercept(1),slope(2),intercept(2),beta(2),beta(1),initratio,'VariableNames',head1);
writetable(prop,[fol1 'graphproperties.xls']);
```

V.3 For side view

V.3.0 sideview.m

```
clc;
clear;
close all;

path = pwd;                                                  % path of current file
fol = [path '/cropped/'];                                   % path of data folders

```

```
8
9  % Naming Conventions_____________________________________________________
10 colorim = ['1DSC_';'1DSC_'];                                  % 1 balls, 2 films
11 binim = ['bb'];                                                % 1 balls, 2 films
12 detectim = ['eb';'ef'];                                        % 1 balls, 2 films
13 excelname = ['b.ods' ;'f.ods'];                                % crude result saving file
14
15 % Creates folder to save data as data%d inside ../cropped/
16 for k= 1:20
17     if 7~=exist([fol 'data' int2str(k)],'dir')
18         mkdir ([fol 'data' int2str(k)])
19         fol1 = [fol 'data' int2str(k) '/'];
20         break
21     end
22 end
23
24 colorimlis = [dir(fullfile(fol, [colorim(1,:) '*.tif'])) dir(fullfile(fol, [colorim(1,:) '*.tif']))];    % [ball_im_list  film_im_list]
25 binimlis = [dir(fullfile(fol, [binim(1,:) '*.tif']))];         % [ball_binim_list  film_binim_list]
26
27
28 count=1;   % count flag
29 for i=1:length(colorimlis(:,1))
30     for l = 1:2
31         im=imread([fol colorimlis(i,l).name]);
32         im3=imsharpen(im(:,:,1));
33         if l ==1
34             % Detecting Ball
35             imb = imread([fol binimlis(i,l).name]);
36             detect = regionprops('table',imb,'Centroid','MajorAxisLength','MinorAxisLength','Orientation','Eccentricity','Area');
37             bestFits = [detect.Centroid(:,1) detect.Centroid(:,2) detect.MajorAxisLength detect.MinorAxisLength detect.Orientation
38             detect.Area]; % this is just to convert table format of detect to matrix form
```

```
        [value,index] = max(bestFits(:,6));%finds maximum area detected ellipse
        % Ploting ball
        implot = figure;
        imshow(im)
        t = linspace(0,2*pi,200); % line 51 to 63 is drawing the ellipse
        hold on
        a = bestFits(index,3)/2;
        b = bestFits(index,4)/2;
        Xc = bestFits(index,1);
        Yc = bestFits(index,2);
        phi = deg2rad(-bestFits(index,5));
        x = Xc + a*cos(t)*cos(phi) - b*sin(t)*sin(phi);
        y = Yc + a*cos(t)*sin(phi) + b*sin(t)*cos(phi);
        plot(x,y,'g','Linewidth',1)
        hold off
        imwrite(imb,[fol1 detectim(l,:) binimlis(i,l).name]);
        saveas(implot,[fol1 detectim(l,:) colorimlis(i,l).name]);
        out=[str2double(colorimlis(i).name(6:9)) bestFits(index,1) bestFits(index,2) bestFits(index,3) bestFits(index,4)
        bestFits(index,5)]; % [ image_no. x0 y0 a b alpha ]
        dlmwrite([fol1 excelname(l,:)],out,'-append');
    elseif l ==2
        % Detection of end points of the film
        found =0;
        for s = 180:300                                          % Set first point detection cropping
            back = im3(3,s);
            [v,in] = max(im3(1:(length(im3(:,s))/5),s));
            if and(v-back>20,found==0)                      % Set threshhold for detection
                first = [s,in];
                found = 1;
            end
        end
```

```
            for s = 600:-1:500                                          % Set last point detection cropping
                back = im3(3,s);
                [v,in] = max(im3(1:(length(im3(:,s))/5),s));
                if and((v-back)>150,found==1)                    % Set threshhold for detection
                    last = [s,in];
                    found = 2;
                end
            end
            alphaf = atan2((bestFits(index,2)-first(2)),(bestFits(index,1)-first(1)));
            alphal = atan2((bestFits(index,2)-last(2)),(bestFits(index,1)-last(1)));
            % Ploting film
            implot = figure;
            imshow(im)% on top of the image which you want to draw detected ellipse
            t = linspace(alphal,alphaf,last(1)-first(1)); % line 51 to 63 is drawing the ellipse
            hold on
            a = bestFits(index,3)/2;
            b = bestFits(index,4)/2;
            Xc = bestFits(index,1);
            Yc = bestFits(index,2);
            phi = deg2rad(-bestFits(index,5));
            rthe = a.*b./(((b.*cos(t-phi)).^2 + (a.*sin(t-phi)).^2).^0.5);
            x = Xc - rthe.*cos(t);
            y = Yc - rthe.*sin(t);
            scatter(x,y,3,'green','filled')
            scatter([first(1),last(1)],[first(2),last(2)], 3,'white','filled')
            hold off
%             f = @(t) sqrt((a*cos(t)).^2 + (b*sin(t)).^2 );
%             compan = abs(integral(f,alphal,alphaf))
            eucdis = sqrt((first(2)-last(2))^2 + (first(1)-last(1))^2 );
            compmaj = a*asin(eucdis/(2*a));                                 % Compansating as circular film
            saveas(implot,[fol1 detectim(l,:) colorimlis(i,l).name]);
```

```
            out=[str2double(colorimlis(i).name(6:9)) first(1) first(2) last(1) last(2) compmaj]; % [ image_no. xf yf xl yl film_dia]
            dlmwrite([fol1 excelname(1,:)],out,'-append');
        end
    end
    count=count+1
    close all;
end

% notification music
load handel.mat;
nBits = 16;
sound(y,Fs,nBits);
```

V.3.0 sideanalysis.m

```
clc;
clear;
close all;
% Selecting the data folder to analyze_____________________________________
path = pwd;                                                    % path of current file
fol = [path '/cropped/'];                                      % path of data folders
files = dir(fol);
for i= 1: length( [files.isdir])
    subFolders1 = files(i).isdir;
    if subFolders1==1
        subFolders = files(i).name;
        disp(subFolders)
    end
end
prompt = 'Which folder do you want to analyze? (as dataint):';
```

```
data = input(prompt,'s');
fol1 = [fol data '/'];                                                    % path of data files


% Reading data files_____________________________________________________________________________________________
t = dlmread('timestamps.ods');                                  % time stamps file [im.no, YYYY,MM,DD,HH,MM,SS,elapsetime]
b = dlmread([fol1 'b.ods']);                                      % ball maj/min/rad file [image_no. x0 y0 a b alpha]
f = dlmread([fol1 'f.ods']);                                      % film maj/min/rad file [image_no. x0 y0 a b alpha]

compmaj = f(:,6);
time = t(:,8)./3600;


% Naming concentions and labels of plots_____________________________________
figname = ['t_vs_Ra'; 't_vs_Wa'];
pngname = ['t_vs_Ra.png'; 't_vs_Wa.png'];
labels = ['Ra (in pixels)'; 'Wa (in pixels)'];

% Plotting of time Vs ball and time Vs film_________________________________
intercept = [];
slope = [];
Y1 = [b(:,4) compmaj];  % ball and film major axis as 2D array
for j= 1:2% line 83 to 99 saves linear regression of time-vs-ball and time-vs-film
    h(j) = figure;
    X = [ones(length(time),1) time];
    Y = Y1(:,j);
    beta = X\Y;
    linearreg = X*beta;
    scatter(time,Y)
    hold on
    plot(time,linearreg,'--')
```

```
    xlabel('time (in hours)');
    ylabel(labels(j,:))
    legend('Data points',['Linear regression,' ' y-intercept :' num2str(beta(1)) ', slope:' num2str(beta(2))],'Location','northoutside')
    intercept = [intercept beta(1)];
    slope = [slope beta(2)];
    savefig(h(j),[fol1 figname(j,:)])
    saveas(h(j),[fol1 pngname(j,:)])
end

% Normalizing ball and film radius_____________________________
normb = b(:,4)./b(1,4);                                  % b(i,4)/intercept(1)];
normf = compmaj(:)./compmaj(1);                % compmaj(i)/intercept(2)];

% Extracting analyzed data file_____________________________________________________
head={'image_name ', 'Ball_major_axis_Ra','Ball_minor_axis_Rb ',  'Ball_Center_x ', 'Ball_Center_y ', 'compansated_film_Wa ' ,
'normalized_ball_RabyRa0 ', 'norm_film_WabyWa0 ', 'Time_in_hours '}; %  headings for analyzed excel file
out=table(b(:,1),b(:,4) ,b(:,5) ,b(:,2) ,b(:,3) ,compmaj,normb ,normf ,time,'VariableNames',head);
writetable(out,[fol1 'emajdata.xls']);

% Ploting w/w0 Vs Ra/Ra0_____________________________________________________________
normb1=normb(and(normb>=0.0,normb<=1.1));      % Set lower and upper limit
normb2=normb(normb>1.1);                                      % Set upper limit
h(3) = figure;
X = [ones(length(normb1),1) normb1];
beta = X\normf(length(normf)-length(normb1)-length(normb2)+1:length(normf)-length(normb2));
linearreg = X*beta;
scatter(normb1,normf(length(normf)-length(normb1)-length(normb2)+1:length(normf)-length(normb2)))
hold on
plot(normb1,linearreg,'--')
xlabel('Ra/Ra0');
ylabel('Wa/Wa0')
```

```
78 legend('Data points',['Linear regression,' ' y-intercept :' num2str(beta(1)) ', slope:' num2str(beta(2))],'Location','northoutside')
79 savefig(h(3),[fol1 'Ra_by_Ra0_Vs_Wa_by_Wa0'])
80 saveas(h(3),[fol1 'Ra_by_Ra0_Vs_Wa_by_Wa0.png'])
81
82 % Saving analyzed results_____________________________________________________
83 initratio = compmaj(1)/b(1,4);                                          % initial film to ball ratio
84 head1 = {'slope_of_t_Vs_Ra','y_intercept_of_t_Vs_Ra' ,'slope_of_t_Vs_Wa','y_intercept_of_t_Vs_Wa', 'slope_of_Ra_by_Ra0_Vs_Wa_by_Wa0',
85 'y_intercept_of_Ra_by_Ra0_Vs_Wa_by_Wa0','Wa_by_Ra_initial'};
86 prop = table(slope(1),intercept(1),slope(2),intercept(2),beta(2),beta(1),initratio,'VariableNames',head1);
87 writetable(prop,[fol1 'graphproperties.xls']);
```

Bibliography

[1] J. Scott Bunch and Martin L. Dunn. Adhesion mechanics of graphene membranes.

[2] Wikipedia contributors. Gaussian curvature — Wikipedia, the free encyclopedia, 2019. [Online; accessed 3-April-2020].

[3] Kittiwit Matan, Rachel B. Williams, Thomas A. Witten, and Sidney R. Nagel. Crumpling a thin sheet. *Phys. Rev. Lett.*, 88:076101, Jan 2002.

[4] Omer Gottesman, Jovana Andrejevic, Chris H. Rycroft, and Shmuel M. Rubinstein. A state variable for crumpled thin sheets. *Communications Physics*, 1(1):70, 2018.

[5] Raph Levien. The elastica: a mathematical history. Technical Report UCB/EECS-2008-103, EECS Department, University of California, Berkeley, Aug 2008.

[6] Wikipedia contributors. Föppl–von kármán equations — Wikipedia, the free encyclopedia, 2019. [Online; accessed 8-November-2019].

[7] Jacob N. Israelachvili. 17 - adhesion and wetting phenomena. In Jacob N. Israelachvili, editor, *Intermolecular and Surface Forces (Third Edition)*, pages 415 – 467. Academic Press, San Diego, third edition edition, 2011.

[8] Benny Davidovitch, Yiwei Sun, and Gregory M. Grason. Geometrically incompatible confinement of solids. *Proceedings of the National Academy of Sciences*, 116(5):1483–1488, 2019.

[9] Prof.Narayan Menon. Wrinkling mechanics.

[10] Vincent Démery. Advanced mechanics.

[11] William S. Slaughter. *The Linearized Theory of Elasticity.* Birkhäuser Basel, 2002.

[12] Richard Hartley and Andrew Zisserman. *Multiple View Geometry in Computer Vision.* Cambridge University Press, USA, 2 edition, 2003.

[13] Wikipedia contributors. Water gel (plain) — Wikipedia, the free encyclopedia, 2020. [Online; accessed 3-April-2020].

[14] Aditi Chakrabarti, Amir Porat, Elie Raphaël, Thomas Salez, and Manoj K. Chaudhury. Elastowetting of soft hydrogel spheres. *Langmuir*, 34(13):3894–3900, April 2018.

[15] Wikipedia contributors. Polystyrene — Wikipedia, the free encyclopedia, 2020. [Online; accessed 3-April-2020].

[16] Jiangshui Huang. Wrinkling of floating thin polymer films. *Doctoral Dissertations 1896 - February 2014. 195*, 2010.

[17] Arduino camera ir blaster.

[18] Hough transform.

[19] imfindcircles.

[20] regionprops.

[21] Wikipedia contributors. Ellipse — Wikipedia, the free encyclopedia, 2020. [Online; accessed 3-April-2020].

[22] B. Audoly and Y. Pomeau. *Elasticity and Geometry: From hair curls to the nonlinear response of shells*. OUP Oxford, 2010.

[23] Pulkit Kumar. Generalized hook's law.

[24] Jérémy Hure, Benoît Roman, and José Bico. Wrapping an Adhesive Sphere with an Elastic Sheet. *Physical Review Letters*, 106(17):174301, April 2011.

[25] Daniel L. Blair and Arshad Kudrolli. Geometry of crumpled paper. *Phys. Rev. Lett.*, 94:166107, Apr 2005.